Chapter V
Results and Comparisons

In this chapter we will show the testing of Fourier transforms, followed by simulations of magnetic field lines for AR7912. Then we compare these results with data from sources in Chapter III. We will discuss these results along with the conclusions in next chapter.

5.1 Testing the Program

To check for errors and test the Fourier transforms and interpolation in our program, first we generated an electric dipole field from positive and negative charges. Assuming that both charges were under the solar surface ($z < 0$), we calculated the electric field up to the solar surface ($z = 0$) and used the electric field at $z = 0$ as the initial data for testing our program.

Figure 5.1 is the contour plot of the z-component of the electric field in the x-y plane at $z = 0$ before the programming process for testing.

Figure 5.2 is the contour plot of the z-component of the electric field in the x-y plane after rotating and bilinear interpolation from system 1 to system 2 and before the FT program. We used $\beta = 26$ degrees, the same angle that will be used for magnetogram data of October 18^{th}, 1995.

Figure 5.3 is the contour plot of the z-component of the electric field in the x-y plane at $z = 0$ after finishing the program.

From this problem, the contour plots before and after the Fourier transform should be the same. Then Figures 5.2 and 5.3 show that there is a small error from the simulation, which is at an acceptable level.

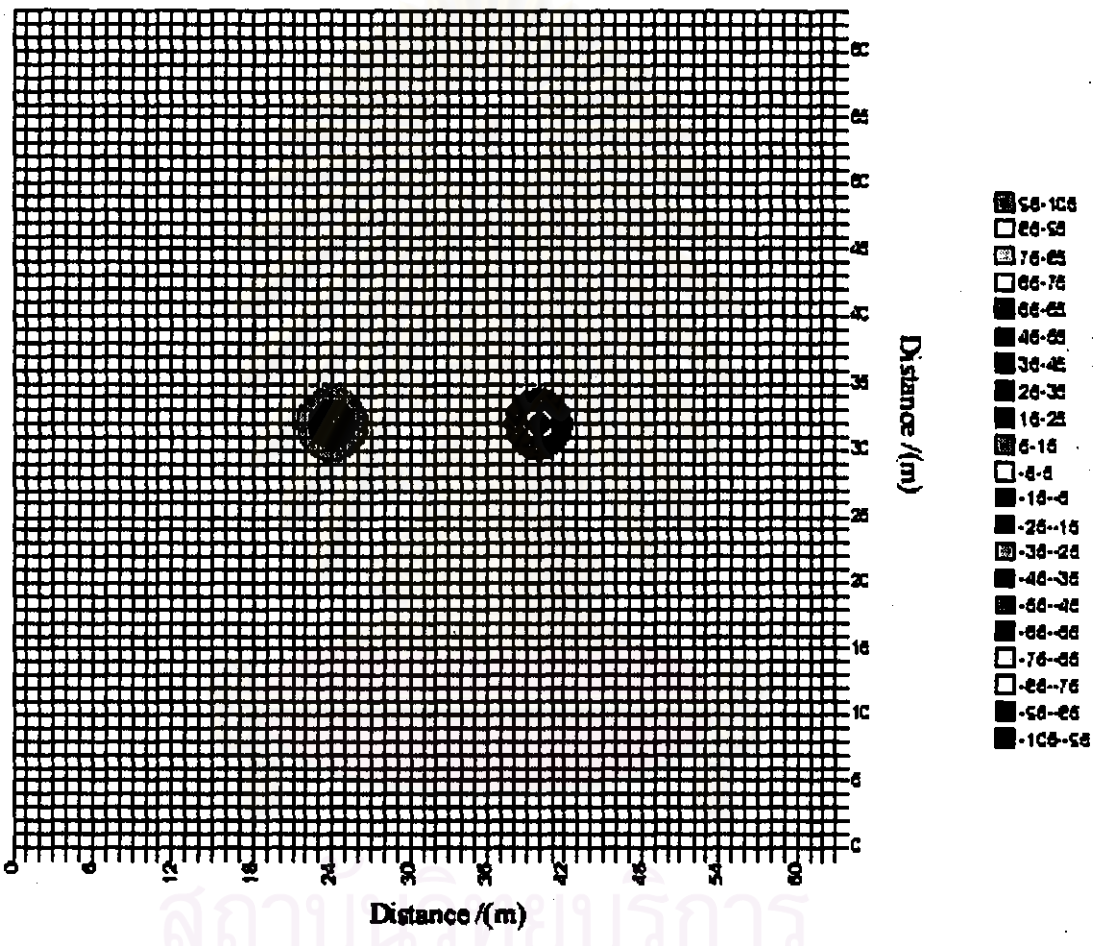

Figure 5.1: The contour plot of the initial z-component electric field data in the x-y plane for testing the program.

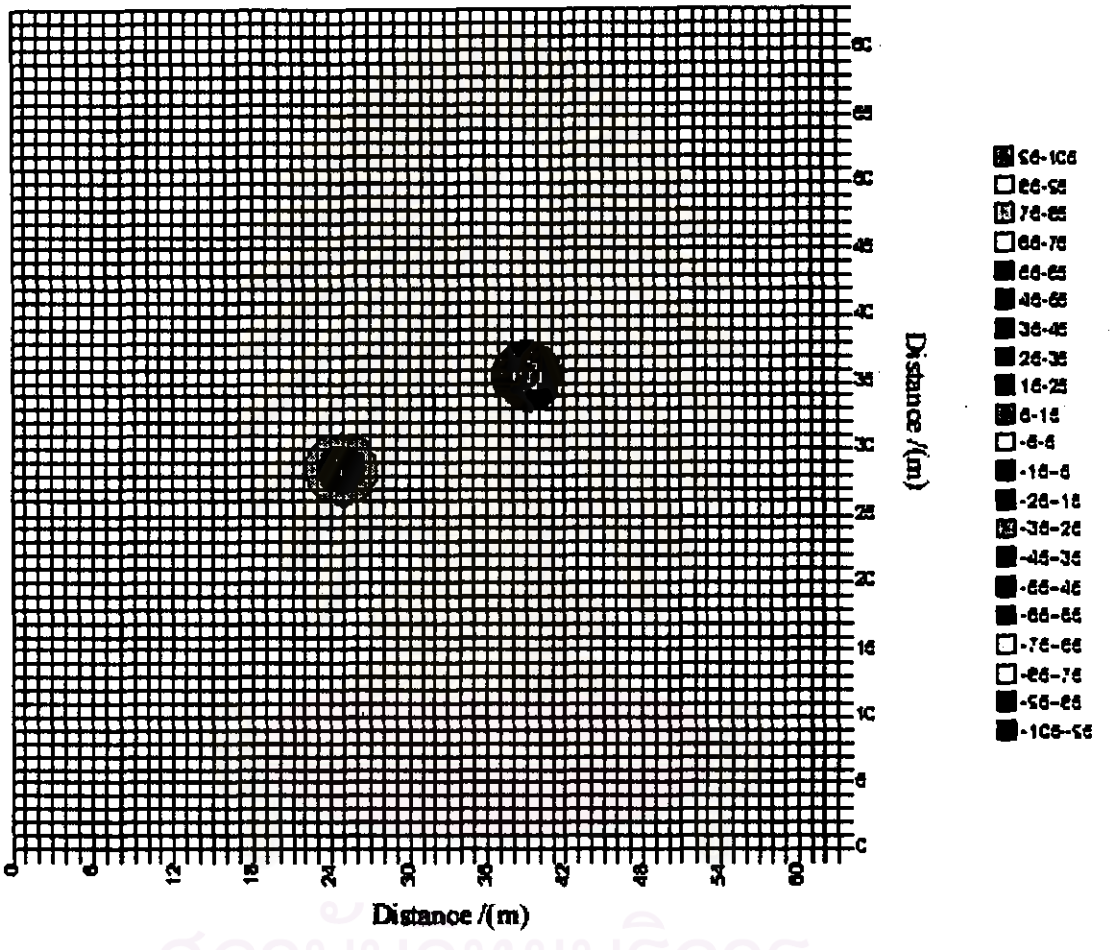

Figure 5.2: The contour plot of the z-component electric field data in the x-y plane for testing the program after rotation and bilinear interpolation.

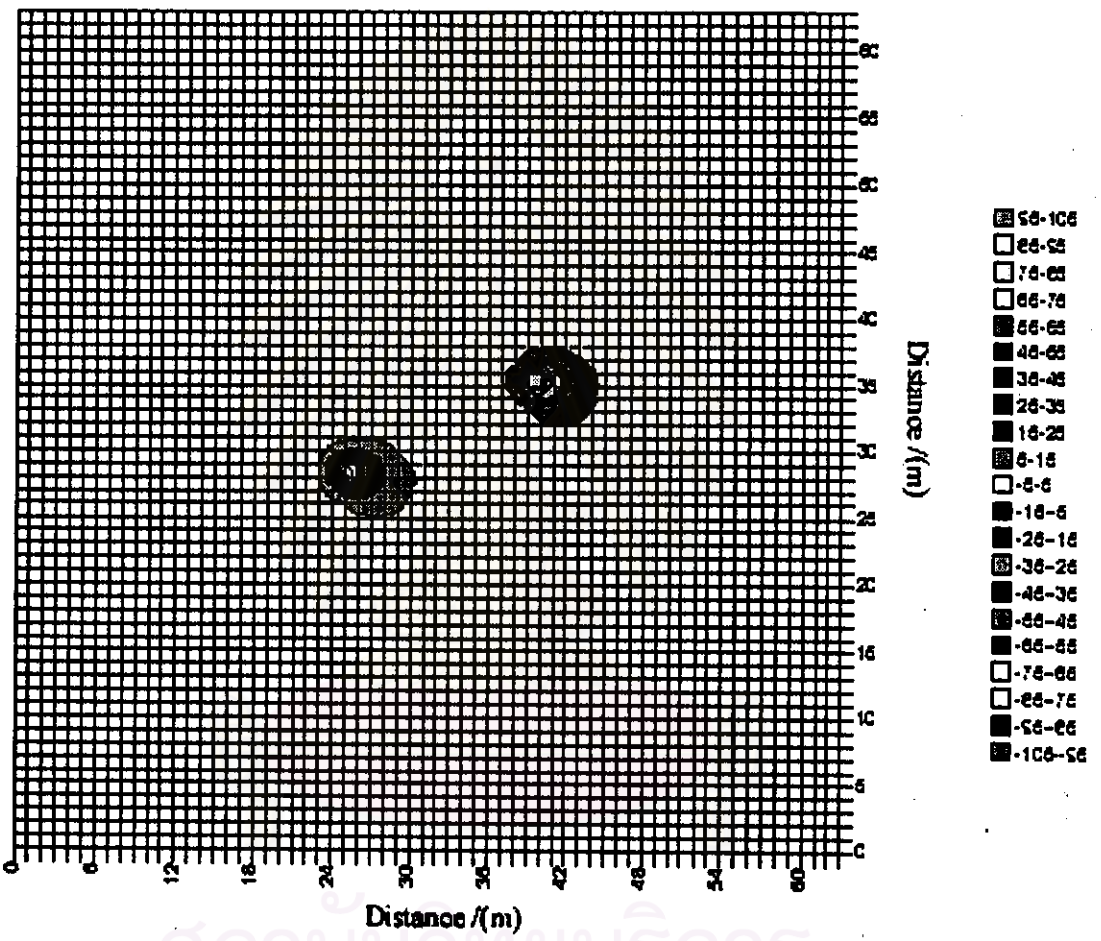

Figure 5.3: The contour plot of the z-component electric field data in the x-y plane when finishing our program after the inverse Fourier transform.

5.2 Simulated Magnetic Field in 3D

For the simulation we used magnetogram data from October 18^{th}, 1995 as initial boundary condition data which gave the magnetic field in the line-of-sight direction (see Figure 3.4). A distance unit which we used in the program to simulate the magnetic field is an "arc second," because as viewed from Earth one arc second on the solar disk is about 3288 km, and the magnetogram data are provided in one-arc-second pixels. Also $1/\alpha$ indicates the scale over which field lines are curved, which can be seen in the x-y vector plots in Figures 5.8 - 5.13.

Figure 5.4 shows a vector plot of the magnetic field on October 18^{th}, 1995 from a simulation in the x-z plane (coordinate system 1) at $\alpha = 0.1$ arc second^{-1}; for simplicity no rotations were performed here. The picture shows the outgoing and incoming magnetic field from one pole to another pole.

Figure 5.5 is a contour plot of the initial magnetic field data from the Kitt Peak magnetogram FITS file at $z = 0$, where here we show the line-of-sight component of the field.

Figure 5.6 is a contour plot of the line-of-sight component of the magnetic field rotated by $\beta = 26°$ at $z = 0$ by using bilinear interpolation before generating magnetic the field in 3D.

Figure 5.7 is a contour plot of the z-component of the magnetic field at $z = 0$ in the x-y plane after finishing the magnetic field generation process.

Figures 5.8 - 5.13 are vector plots showing the characteristics of the magnetic field in the x-y plane situated at 20 arc seconds in height above the photosphere for α = -0.1, 10^{-10}, 0.05, 0.1, and 0.15 arc second^{-1}.

These results give various characteristics of the magnetic field depending on the constant α. If $\alpha > 0$ or $\alpha < 0$ the magnetic field will twist along an S shape or inverse-S shape, respectively.

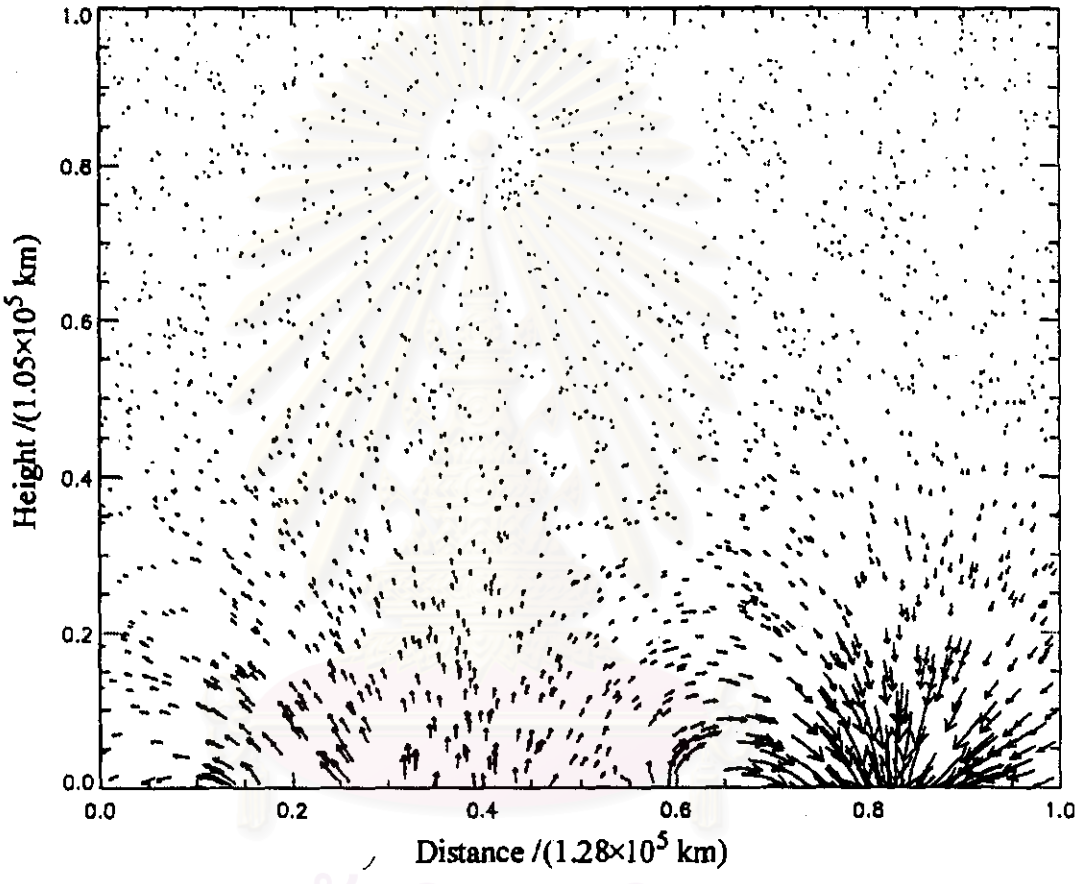

Figure 5.4: Vector plot of the magnetic field on October 18th, 1995 at $\alpha = 0.1$ arc second^{-1} in the x-z plane.

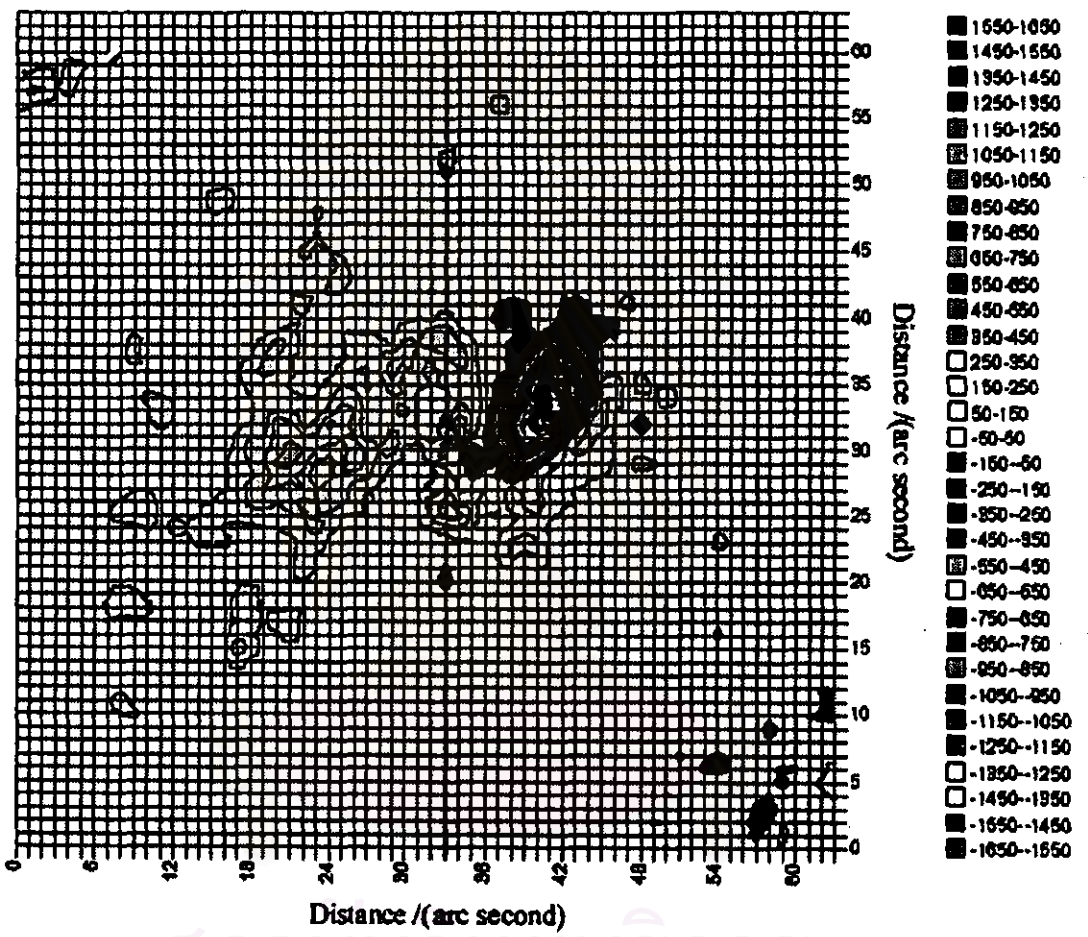

Figure 5.5: Contour plot of initial magnetic field data, B_l (in G), on October 18^{th}, 1995 in the x-y plane.

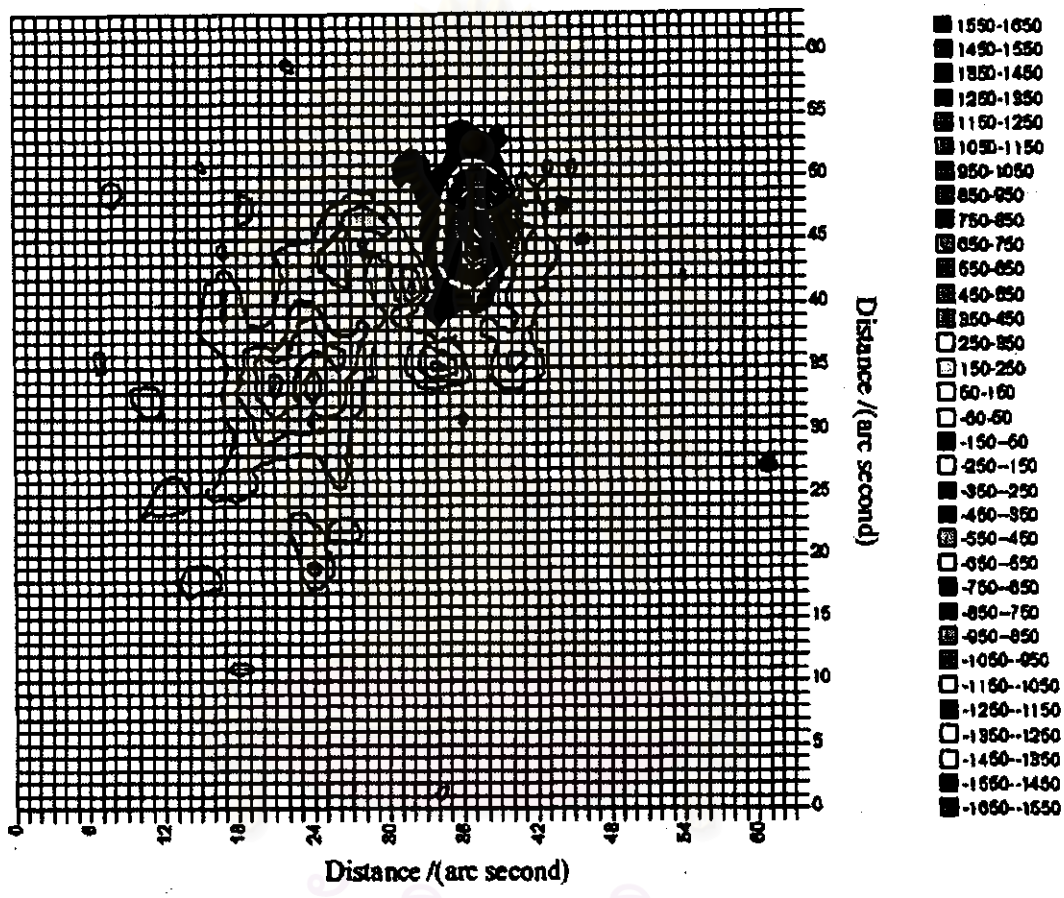

Figure 5.6: Contour plot of B_l (in G) in the x-y plane on October 18^{th}, 1995 at $\alpha = 0.1$ arc second^{-1}, after rotation by $\beta = 26°$.

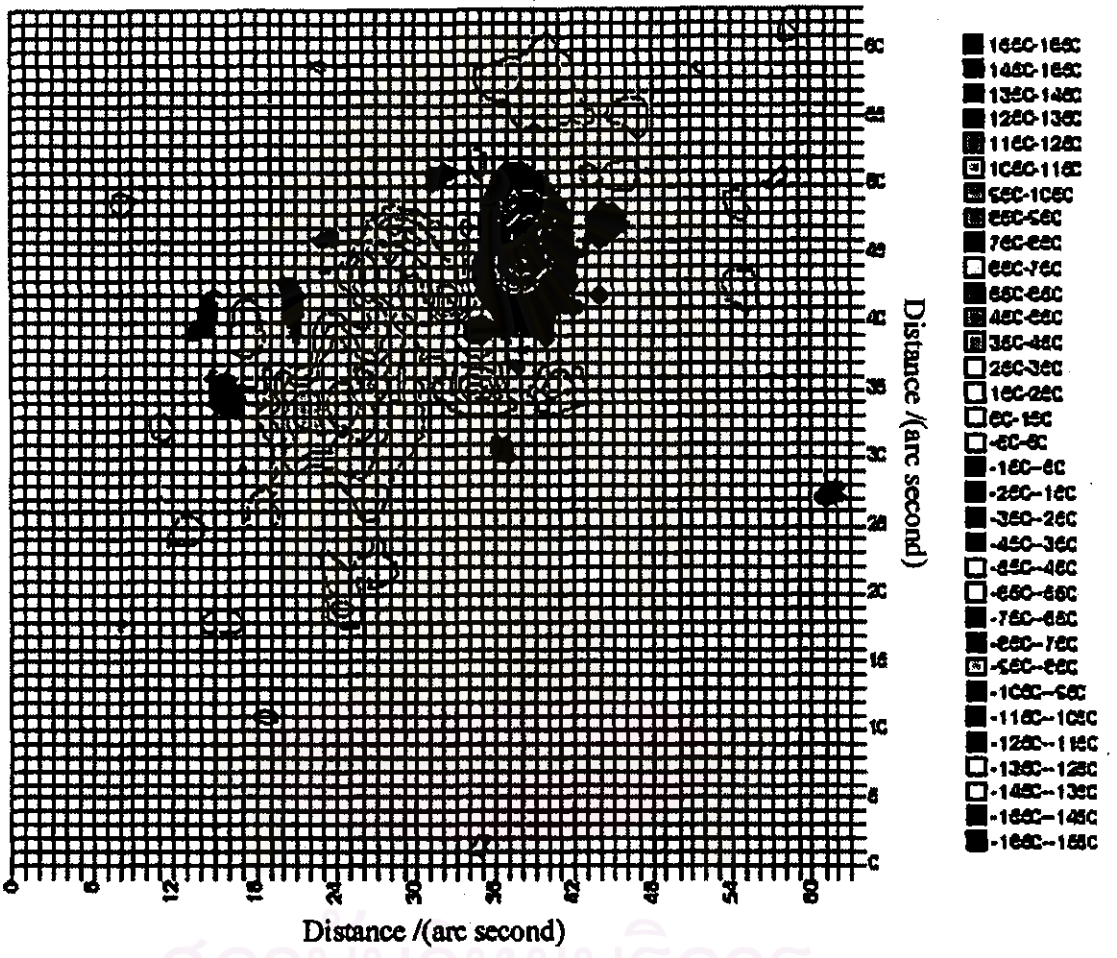

Figure 5.7: Contour plot of B_z (in G) in the x-y plane on October 18^{th}, 1995 at $\alpha = 0.1$ arc second^{-1} after finishing the field simulation program.

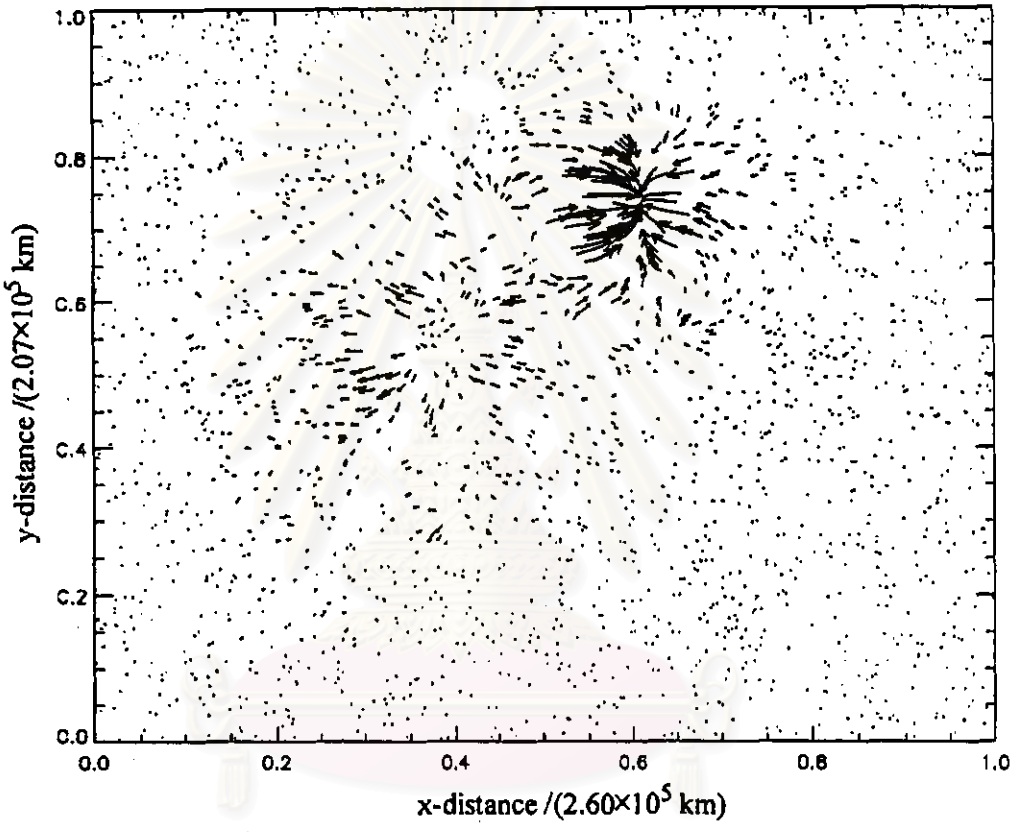

Figure 5.8: Vector plot of the magnetic field in the x-y plane at $z = 0$ and α near 0. Sunspots (x,y) locations are approximately (0.35, 0.55) and (0.60, 0.75) in these units.

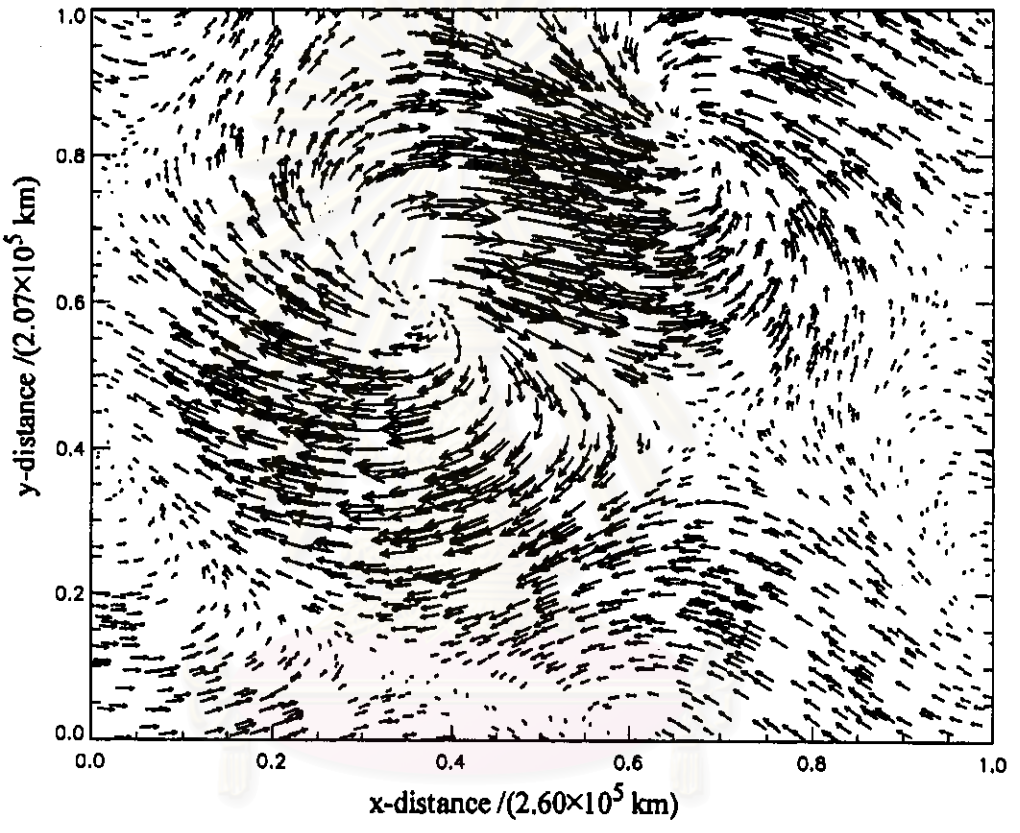

Figure 5.9: Vector plot of the magnetic field in the x-y plane at $z = 20$ arc seconds ($\approx$ 66,000 km) and α = -0.1 arc second^{-1}.

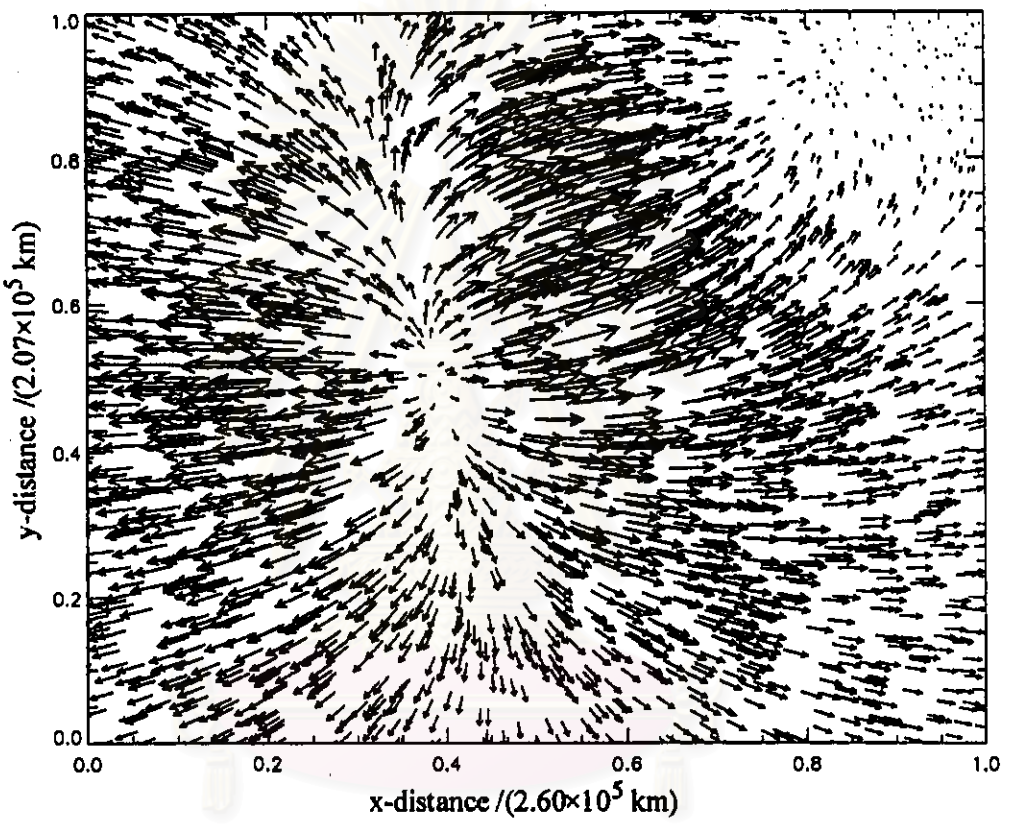

Figure 5.10: Vector plot of the magnetic field in the x-y plane at $z = 20$ arc seconds ($\approx$ 66,000 km) and α near 0.

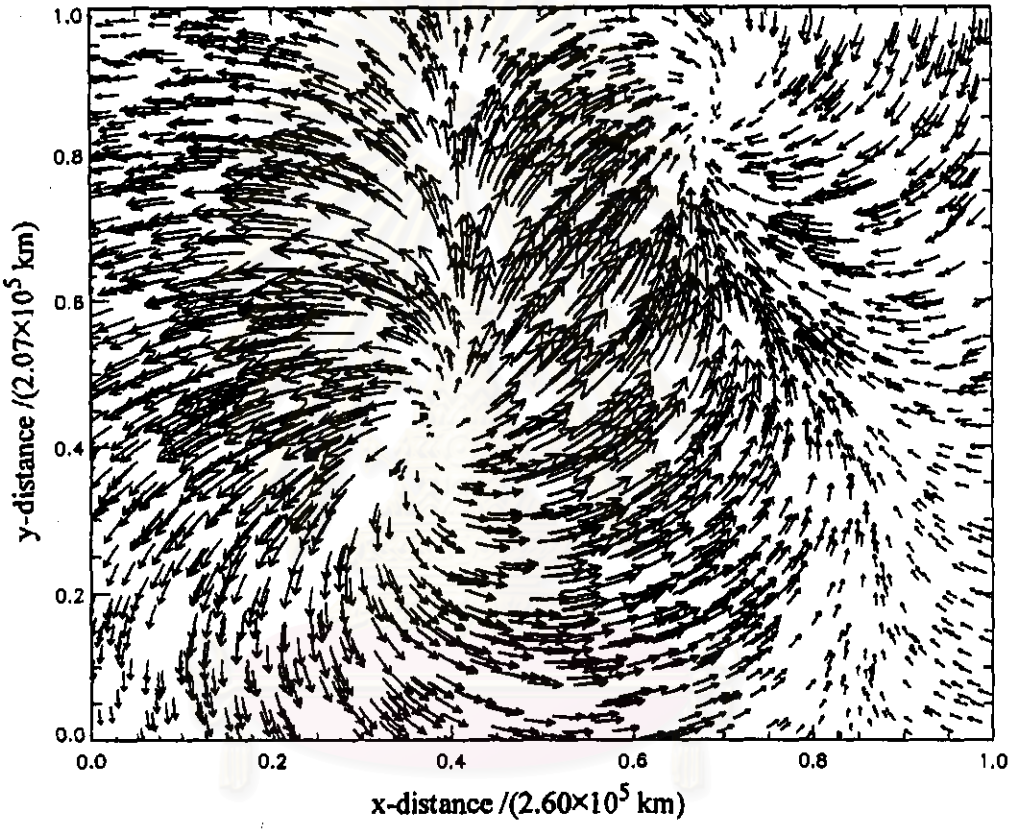

Figure 5.11: Vector plot of the magnetic field in the x-y plane at $z = 20$ arc seconds ($\approx$ 66,000 km) and $\alpha = 0.05$ arc second^{-1}.

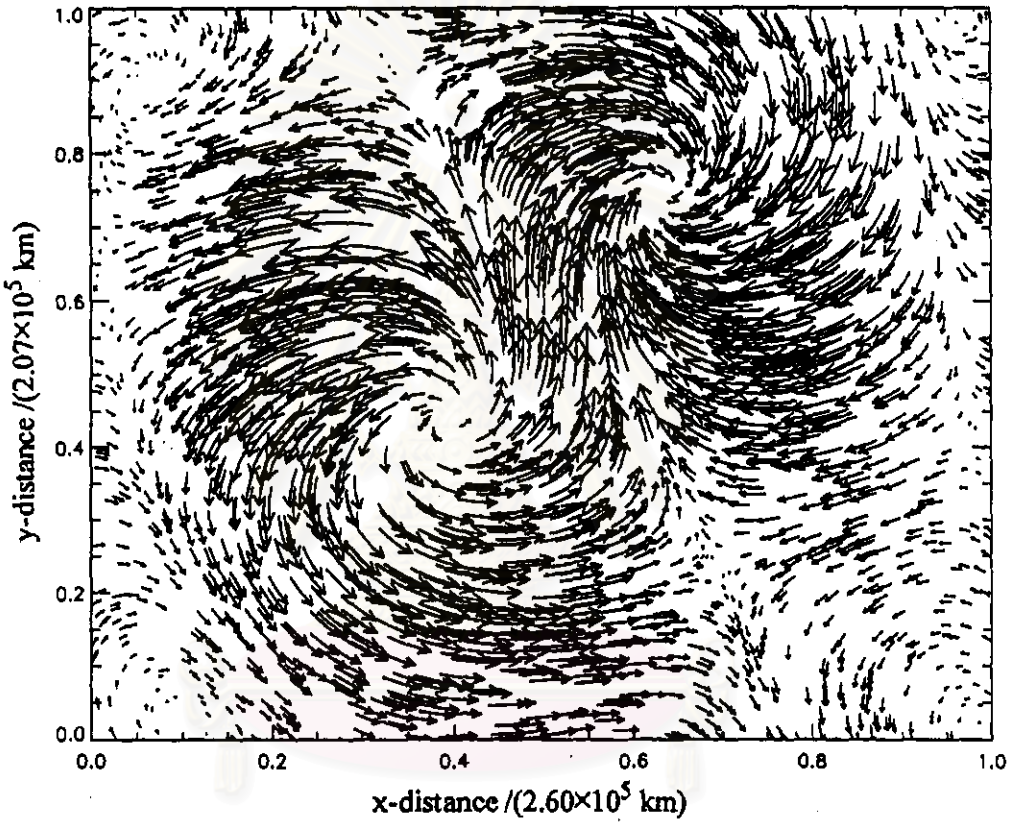

Figure 5.12: Vector plot of the magnetic field in the x-y plane at $z = 20$ arc seconds ($\approx$ 66,000 km) and $\alpha = 0.1$ arc second^{-1}.

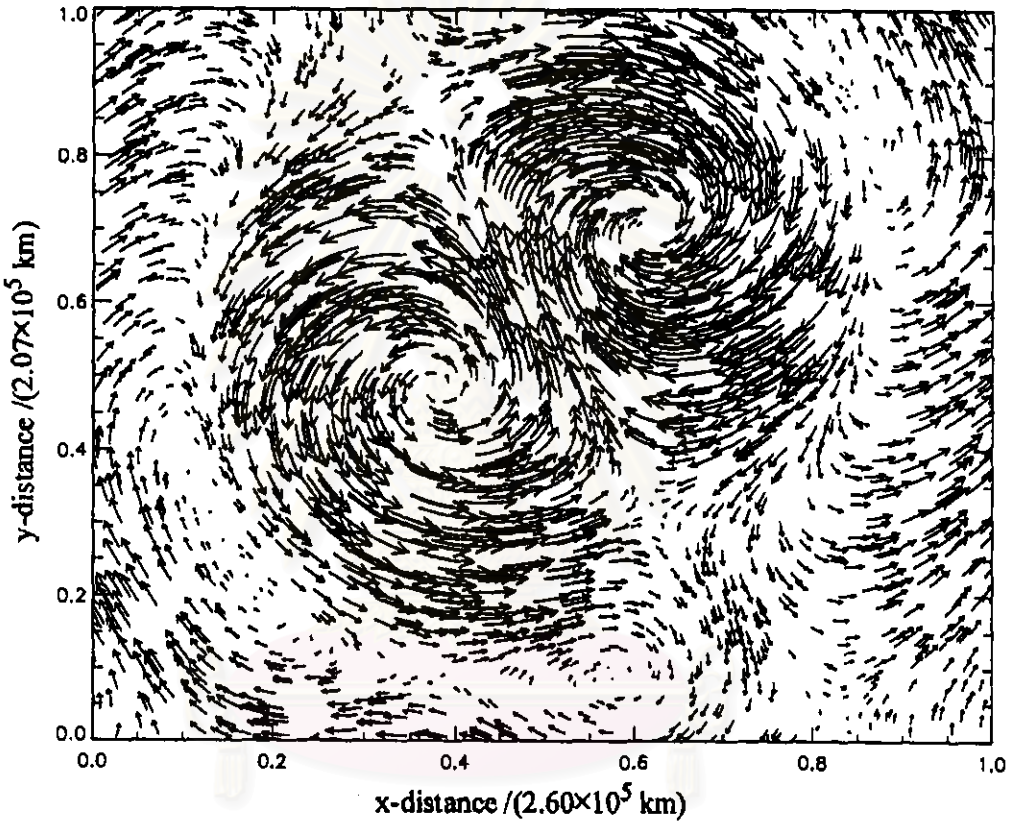

Figure 5.13: Vector plot of the magnetic field in the x-y plane at $z = 20$ arc seconds ($\approx$ 66,000 km) and $\alpha = 0.15$ arc second^{-1}.

5.3 Minimization to Select Initial Points of Visualized Magnetic Field Lines

Before tracing the magnetic field lines for 18^{th} October, 1995, we need to find initial points for field line tracing in our tracing program. First, we selected a plane for selecting the initial points by considering the characteristics of the magnetic field in the vector and contour plots in the previous section. In this we chose an x-z plane halfway between the sunspots, since this plane is perpendicular to the S-shaped magnetic field lines between two magnetic poles and used the method shown in Chapter IV. To trace the magnetic field lines, we used 100 points in the x-z plane at $\alpha = 0.05$, 0.1, and 0.15 arc second^{-1}. After minimization of V (see section 4.4), the density of points will be approximately proportional to the magnitude of the magnetic field component in the y-direction. The boundaries for our minimization were about 20 arc seconds (about 65,700 km) to 63 arc seconds (about 2.07×10^5 km) in the z direction. Trial points position before minimization (chosen by hand) and positions after minimization, which will serve as initial positions for magnetic field line tracing, are shown in Figures 5.14 - 5.19. Notice that after minimization, the points are more evenly spaced, with a density proportional to $|B_y|$, which is concentrated along the main loop at $x \approx 65''$, $z \approx 25''$.

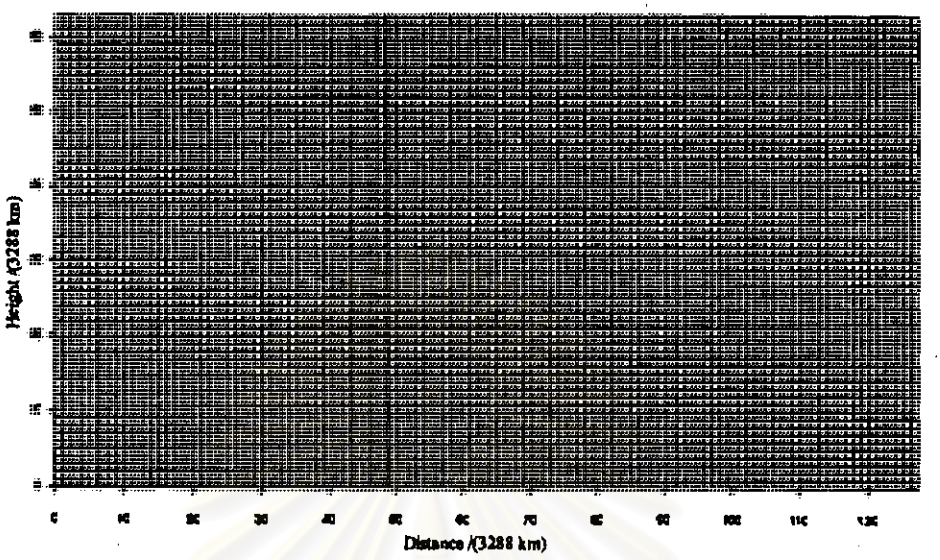

Figure 5.14: Initial x-z points before minimizing V at $\alpha = 0.05$ arc second^{-1}.

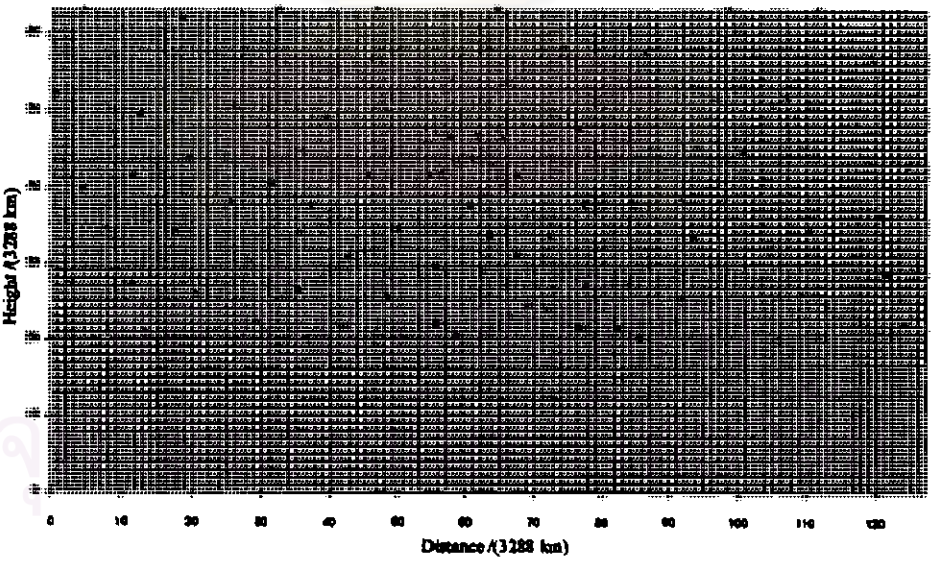

Figure 5.15: Initial x-z points after minimizing V at $\alpha = 0.05$ arc second^{-1}.

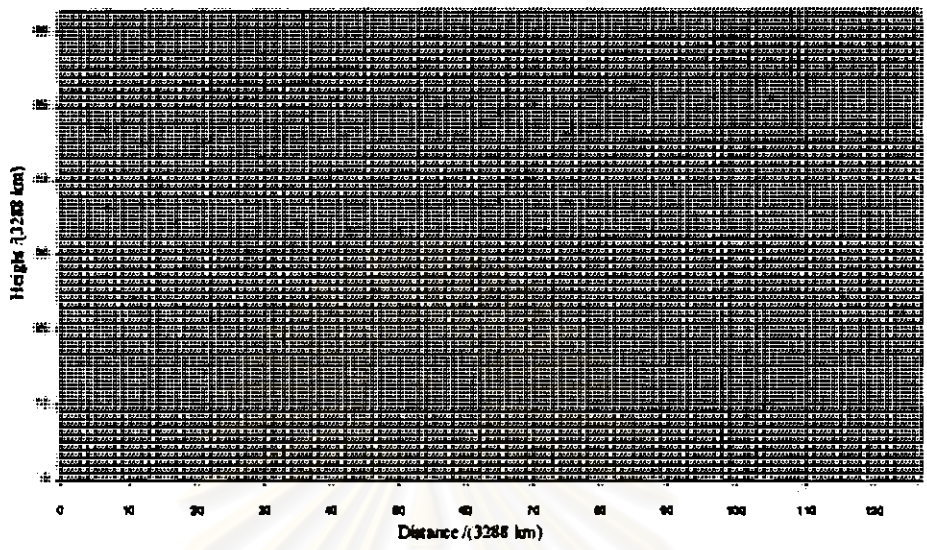

Figure 5.16: Initial x-z points before minimizing V at $\alpha = 0.1$ arc second^{-1}.

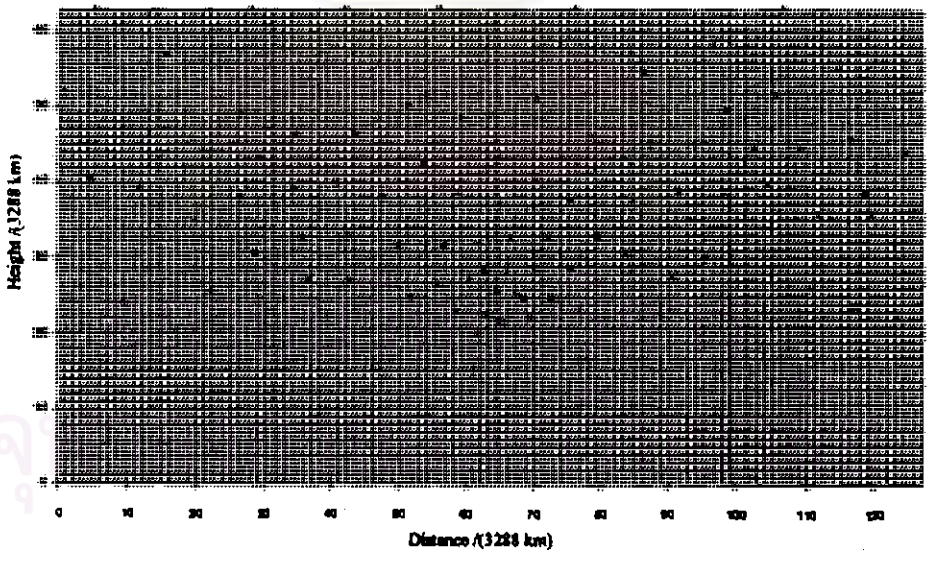

Figure 5.17: Initial x-z points after minimizing V at $\alpha = 0.1$ arc second^{-1}.

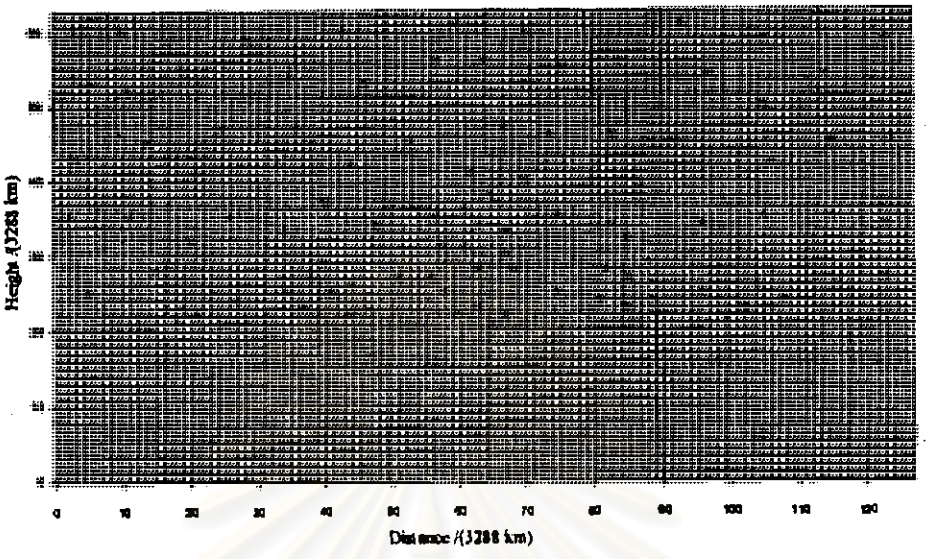

Figure 5.18: Initial x-z points before minimizing V at $\alpha = 0.15$ arc second^{-1}.

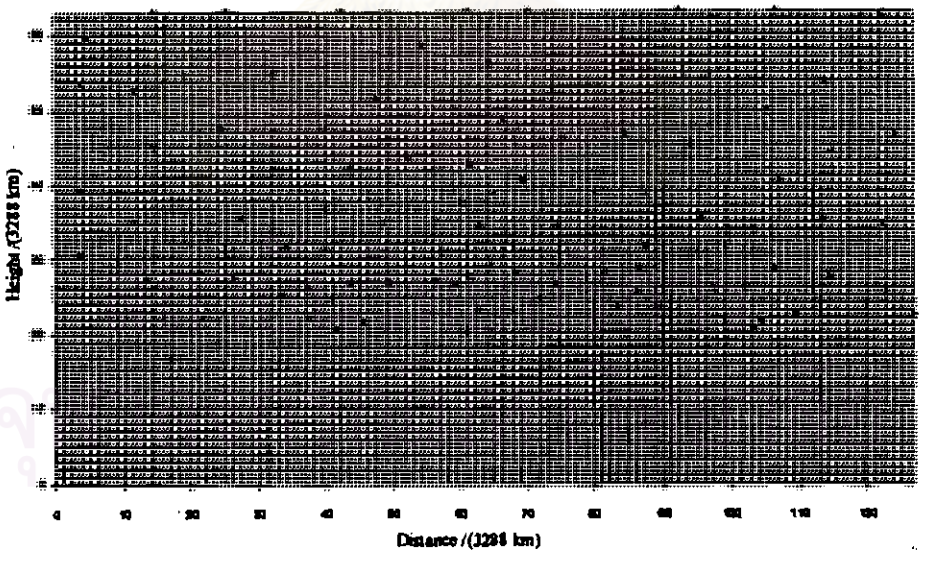

Figure 5.19: Initial x-z points after minimizing V at $\alpha = 0.15$ arc second^{-1}.

5.4 Results of Tracing Magnetic Field Line Results

We show the results of tracing magnetic field lines for our simulations for magnetogram data on 18^{th} October, 1995. We then rotated the resulting field lines to October 15^{th} (15:15:00 UT), 17^{th} (15:34:47 UT), 18^{th} (14:59:24 UT), 20^{th} (15:12:54 UT), 21^{st} (15:40:12 UT), and 24^{th} (3:40:00 UT) using all three values of α. We chose some lines to plot where we expected the middle of the S-shaped magnetic field to pass by observation from the results of the vector plots (see section 5.2) on the solar surface and chose the height (in the z-direction) from observational data. Figures 5.20 - 5.22 show magnetic field lines in three dimensions for October 18^{th} and different values of α, while Figures 5.23 - 5.40 show results for field lines as they would appear as viewed from Earth at various times and for various values of α.

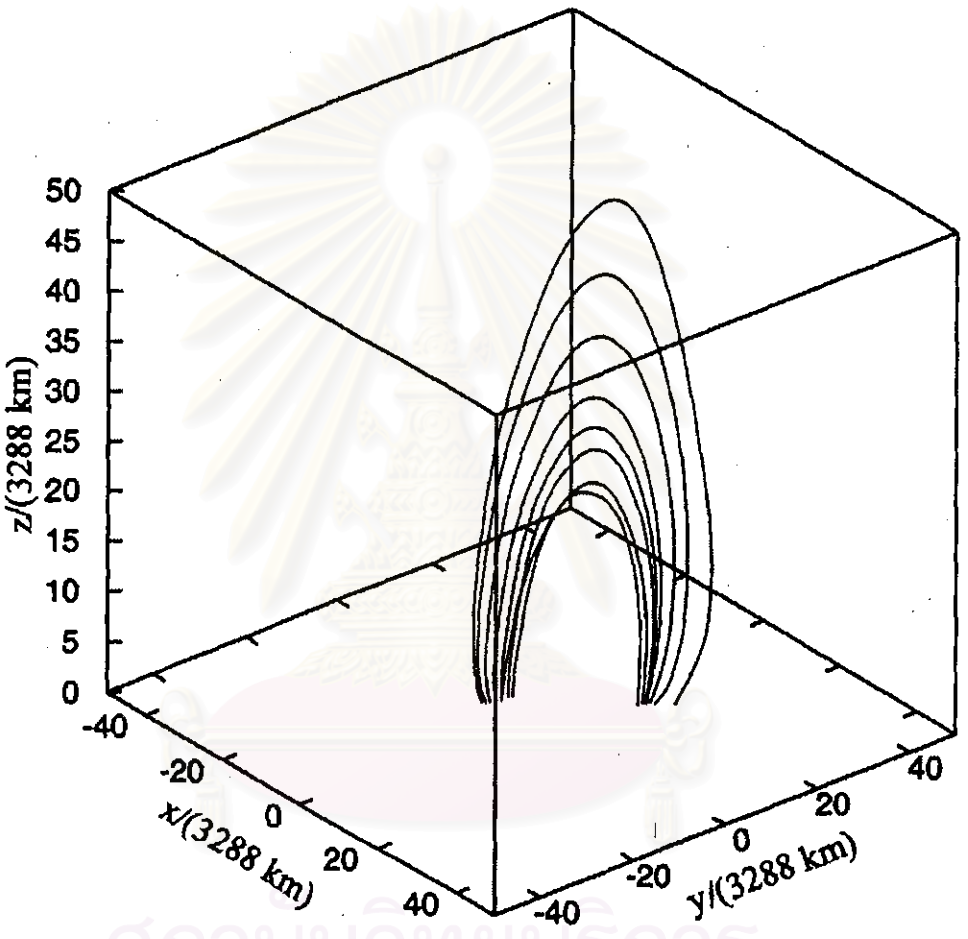

Figure 5.20: The magnetic field lines in 3D at $\alpha = 0.05$ arc second^{-1} for 18^{th} October, 1995.

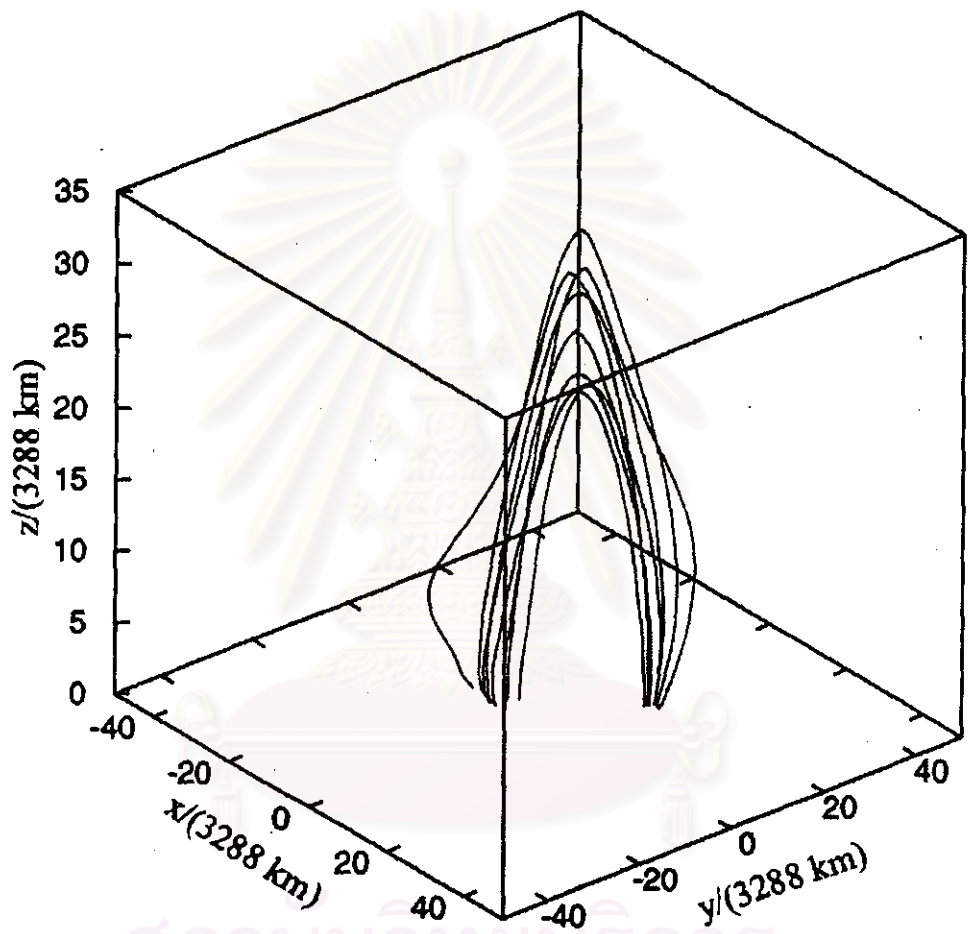

Figure 5.21: The magnetic field lines in 3D at $\alpha = 0.10$ arc second^{-1} for 18^{th} October, 1995.

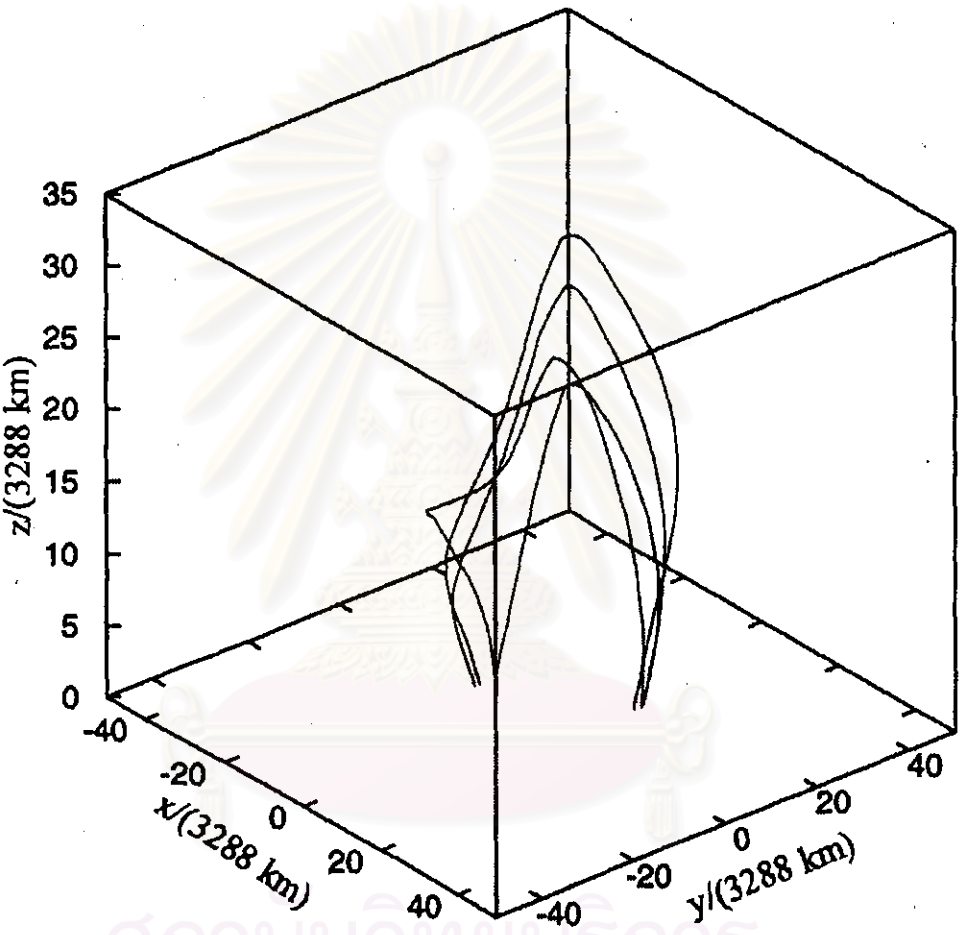

Figure 5.22: The magnetic field lines in 3D at $\alpha = 0.15$ arc second^{-1} for 18^{th} October, 1995.

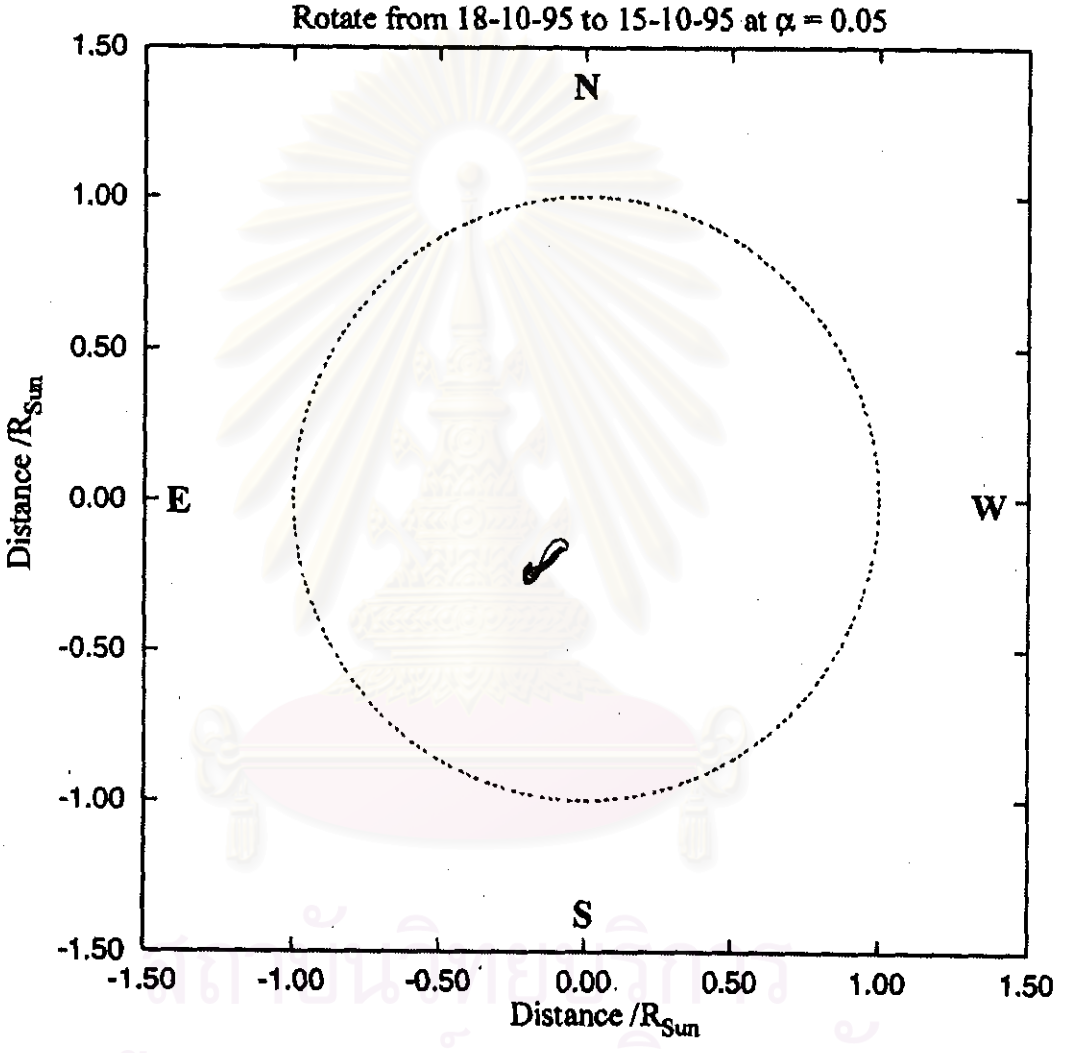

Figure 5.23: Simulation of the magnetic field, rotated from 18-10-95 to 15-10-95, at $\alpha = 0.05$ arc second^{-1}.

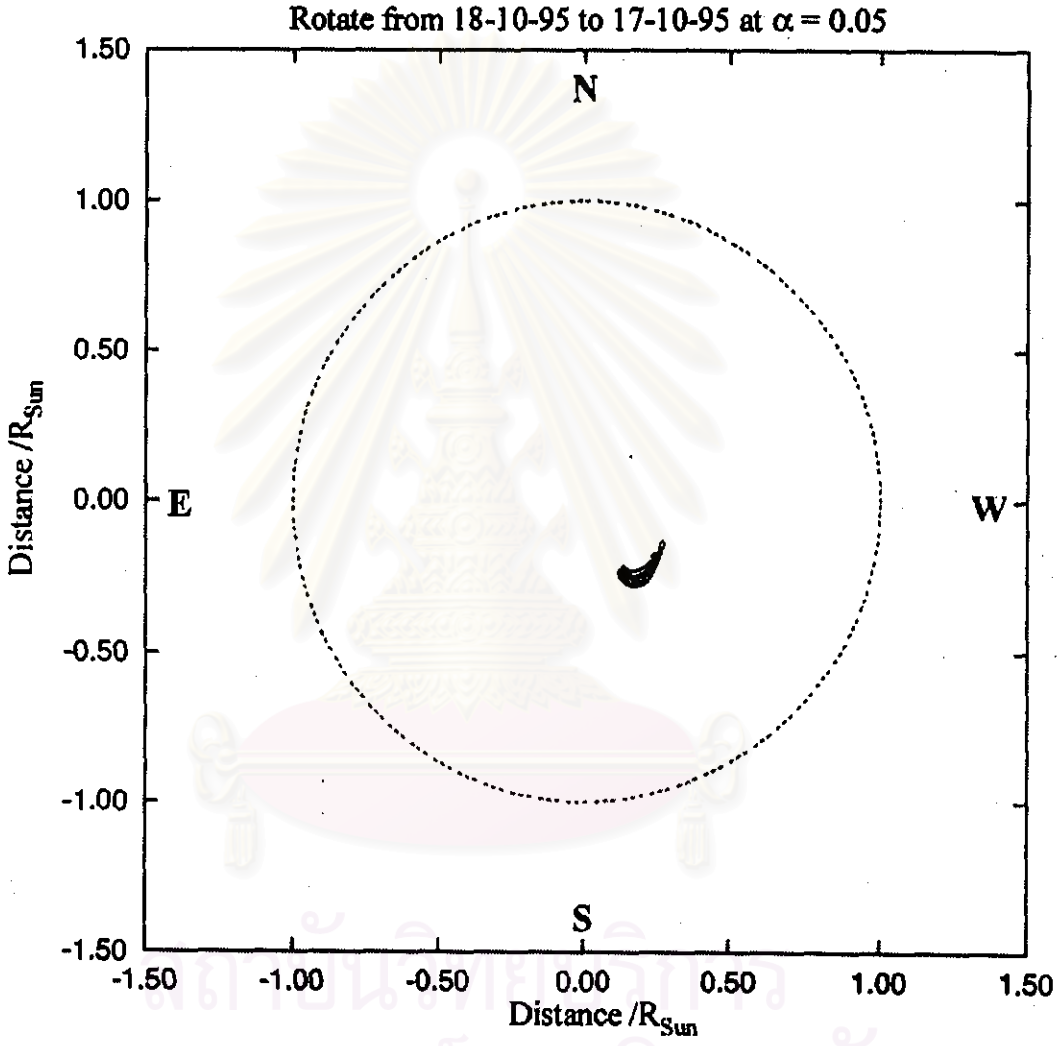

Figure 5.24: Simulation of the magnetic field, rotated from 18-10-95 to 17-10-95, at $\alpha = 0.05$ arc second^{-1}.

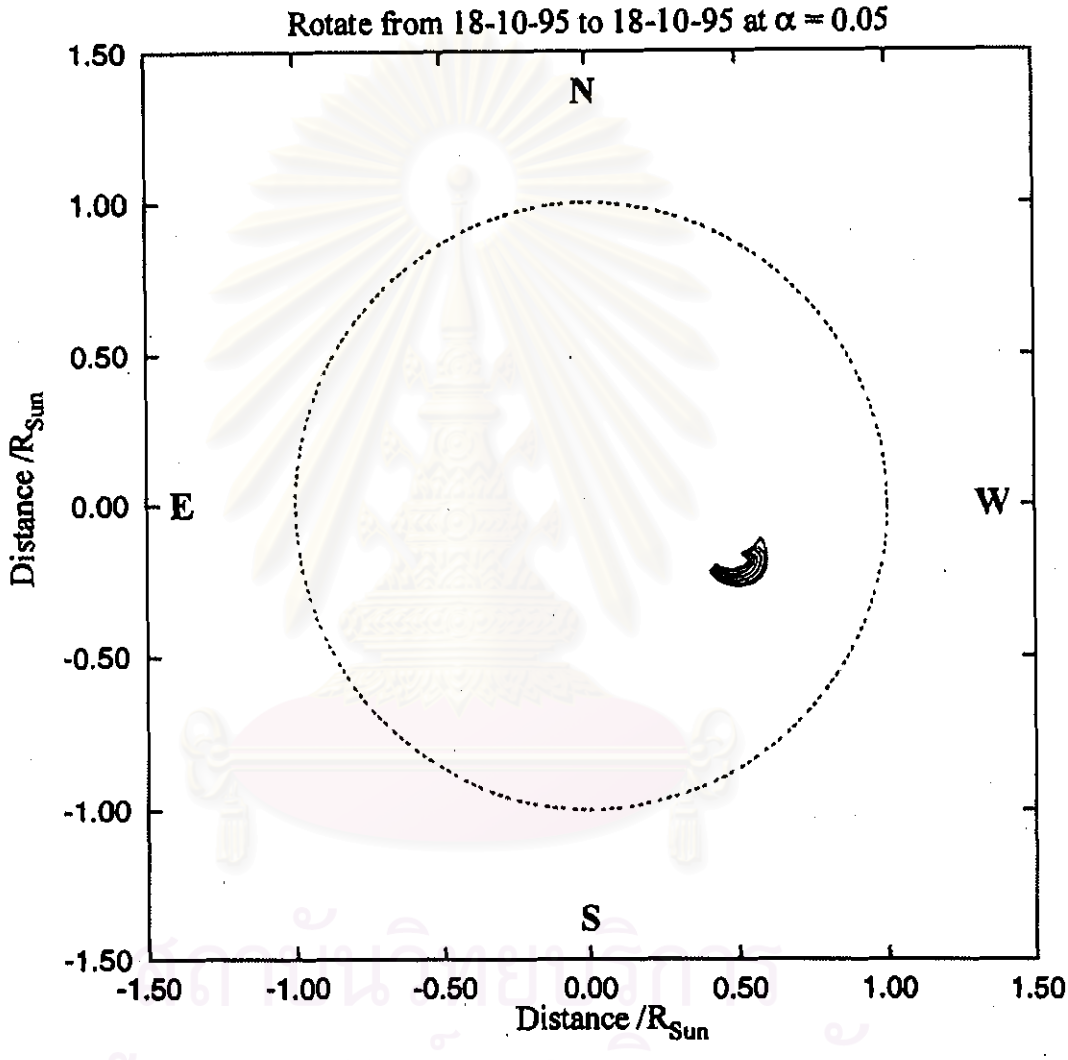

Figure 5.25: Simulation of the magnetic field, rotated from 18-10-95 to 18-10-95, at $\alpha = 0.05$ arc second^{-1}.

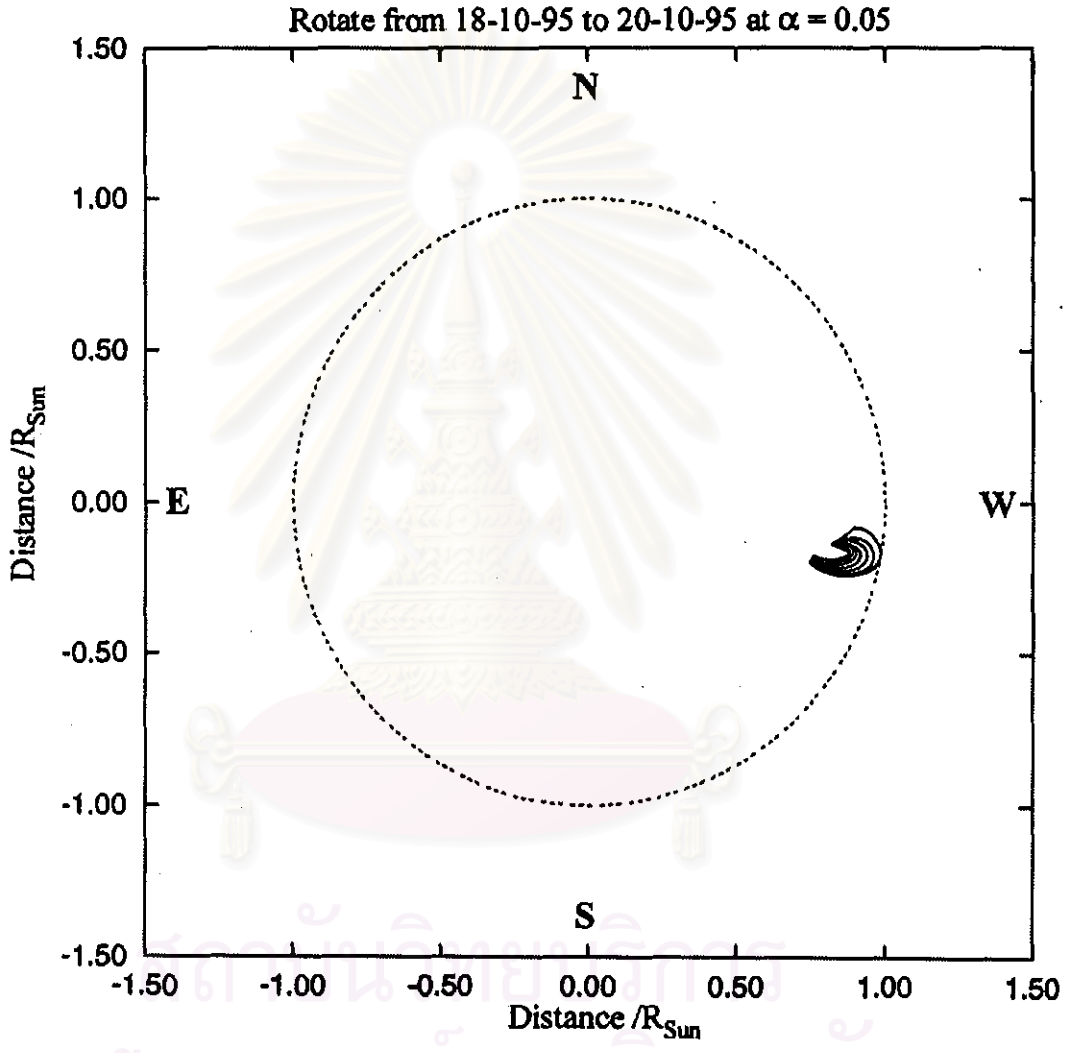

Figure 5.26: Simulation of the magnetic field, rotated from 18-10-95 to 20-10-95, at $\alpha = 0.05$ arc second^{-1}.

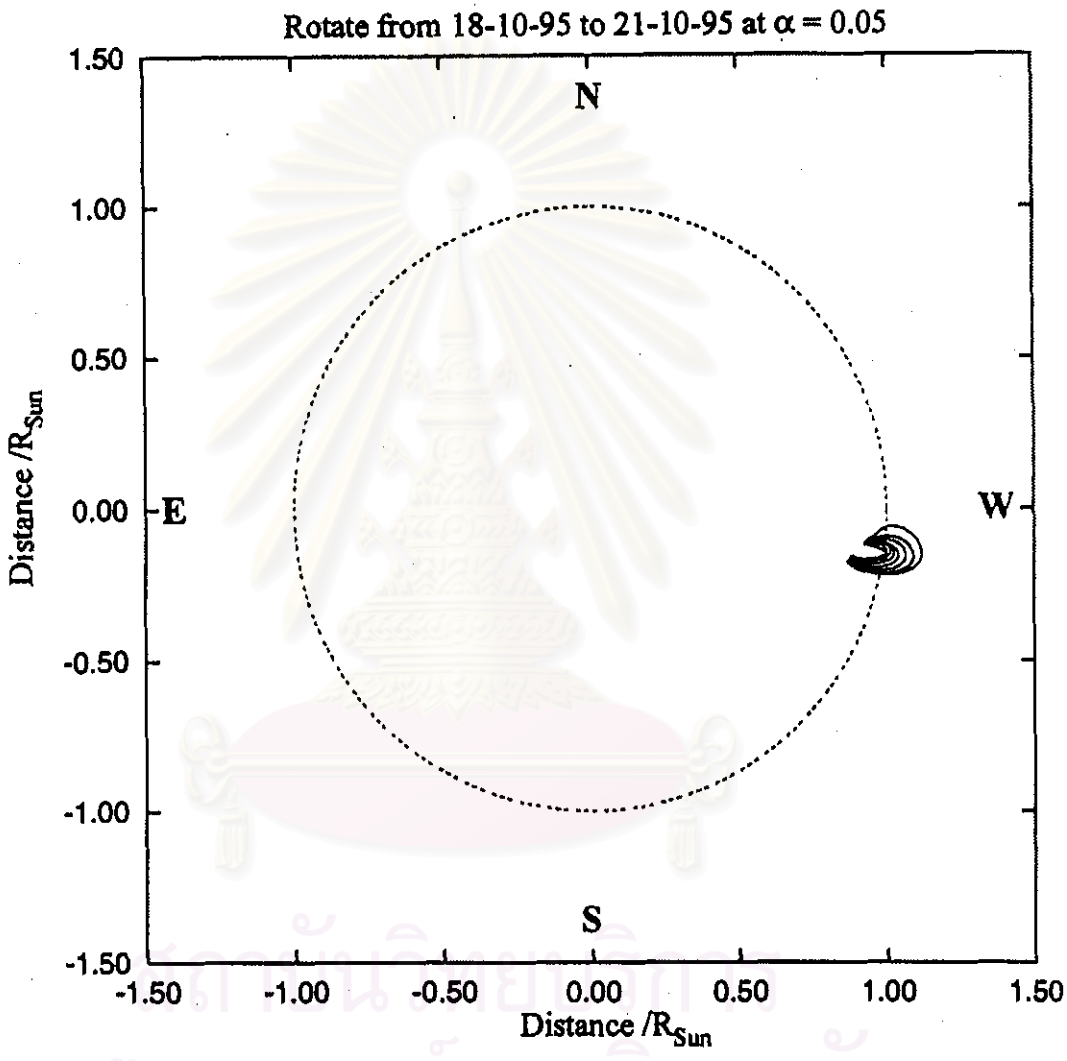

Figure 5.27: Simulation of the magnetic field, rotated from 18-10-95 to 21-10-95, at $\alpha = 0.05$ arc second^{-1}.

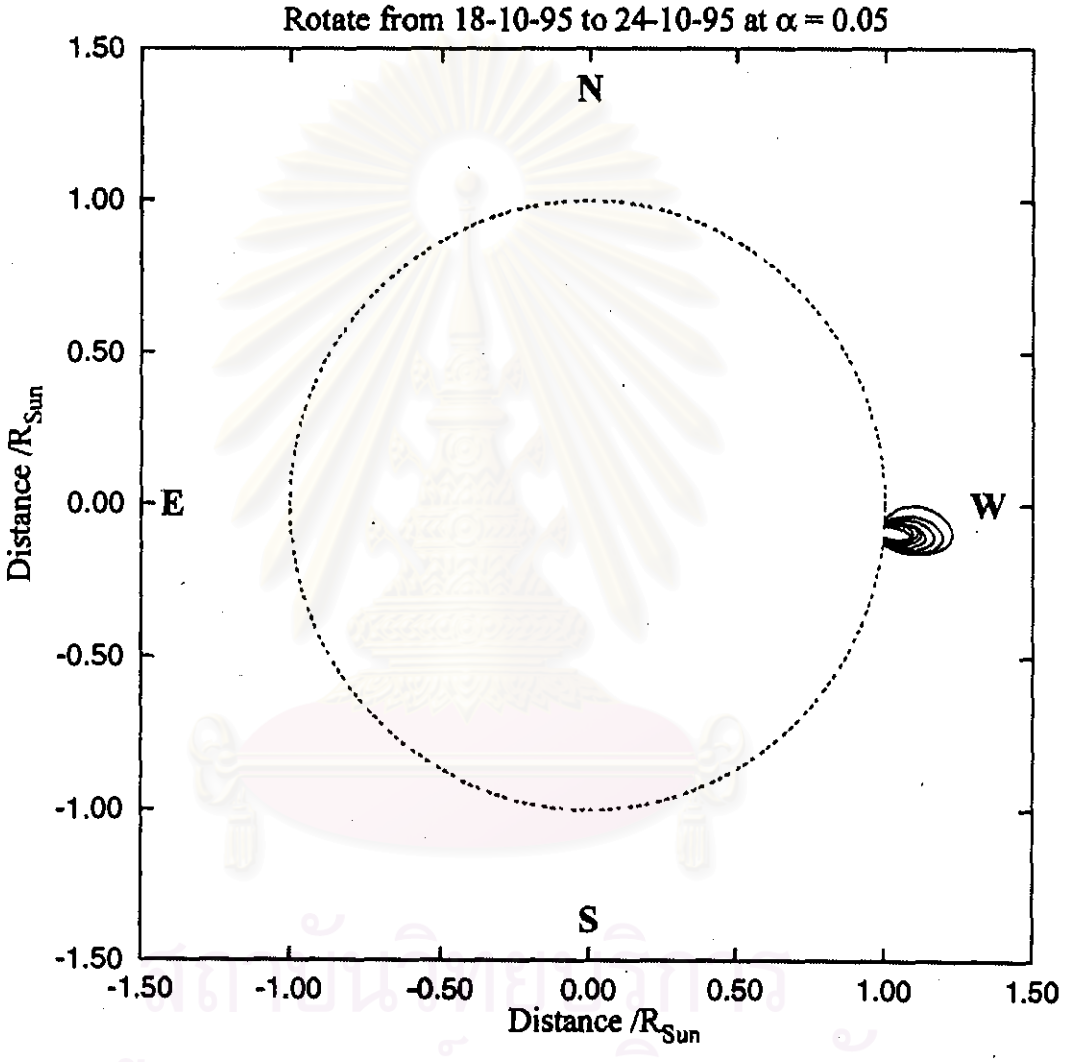

Figure 5.28: Simulation of the magnetic field, rotated from 18-10-95 to 24-10-95, at $\alpha = 0.05$ arc second^{-1}.

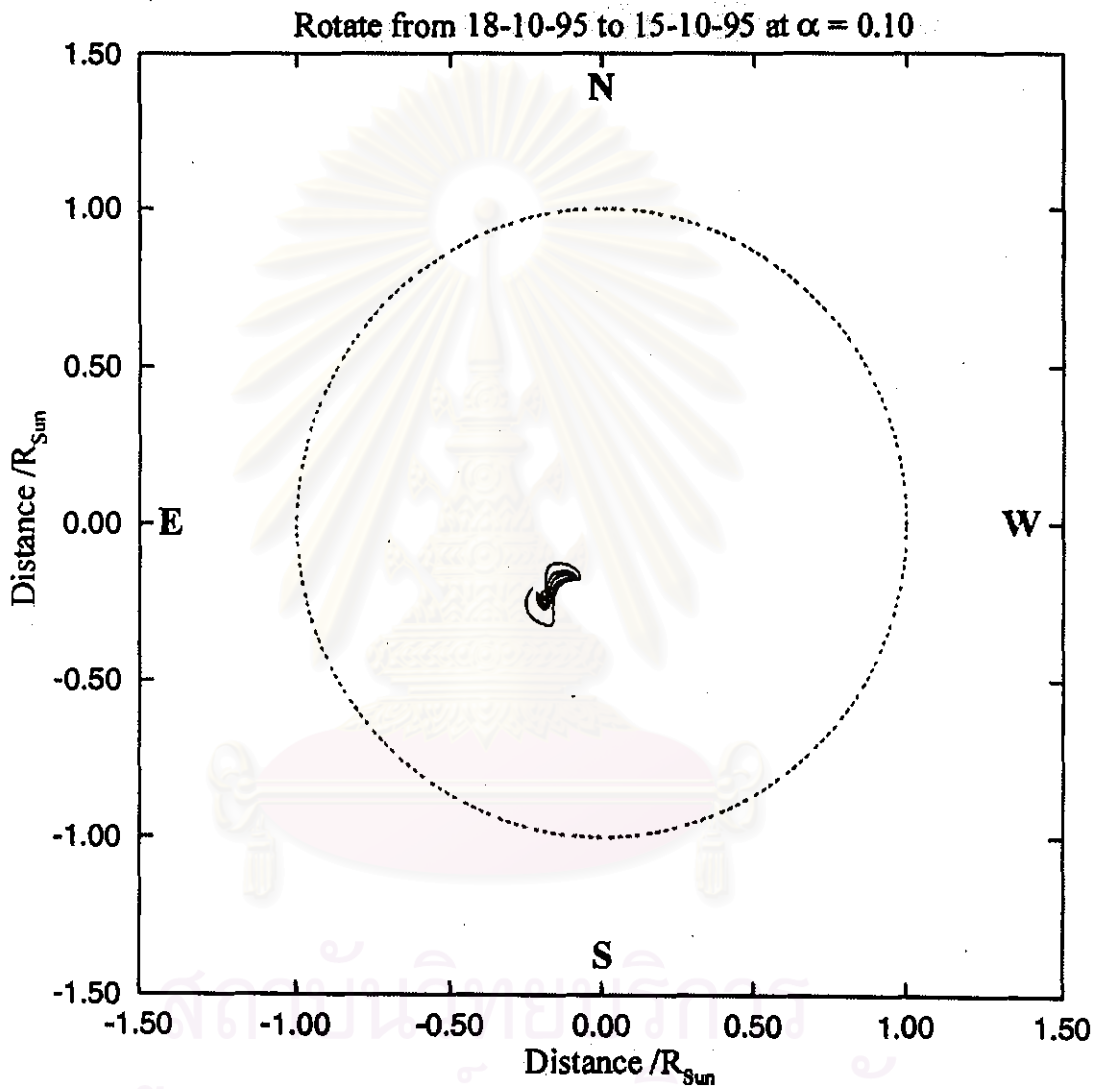

Figure 5.29: Simulation of the magnetic field, rotated from 18-10-95 to 15-10-95, at $\alpha = 0.10$ arc second^{-1}.

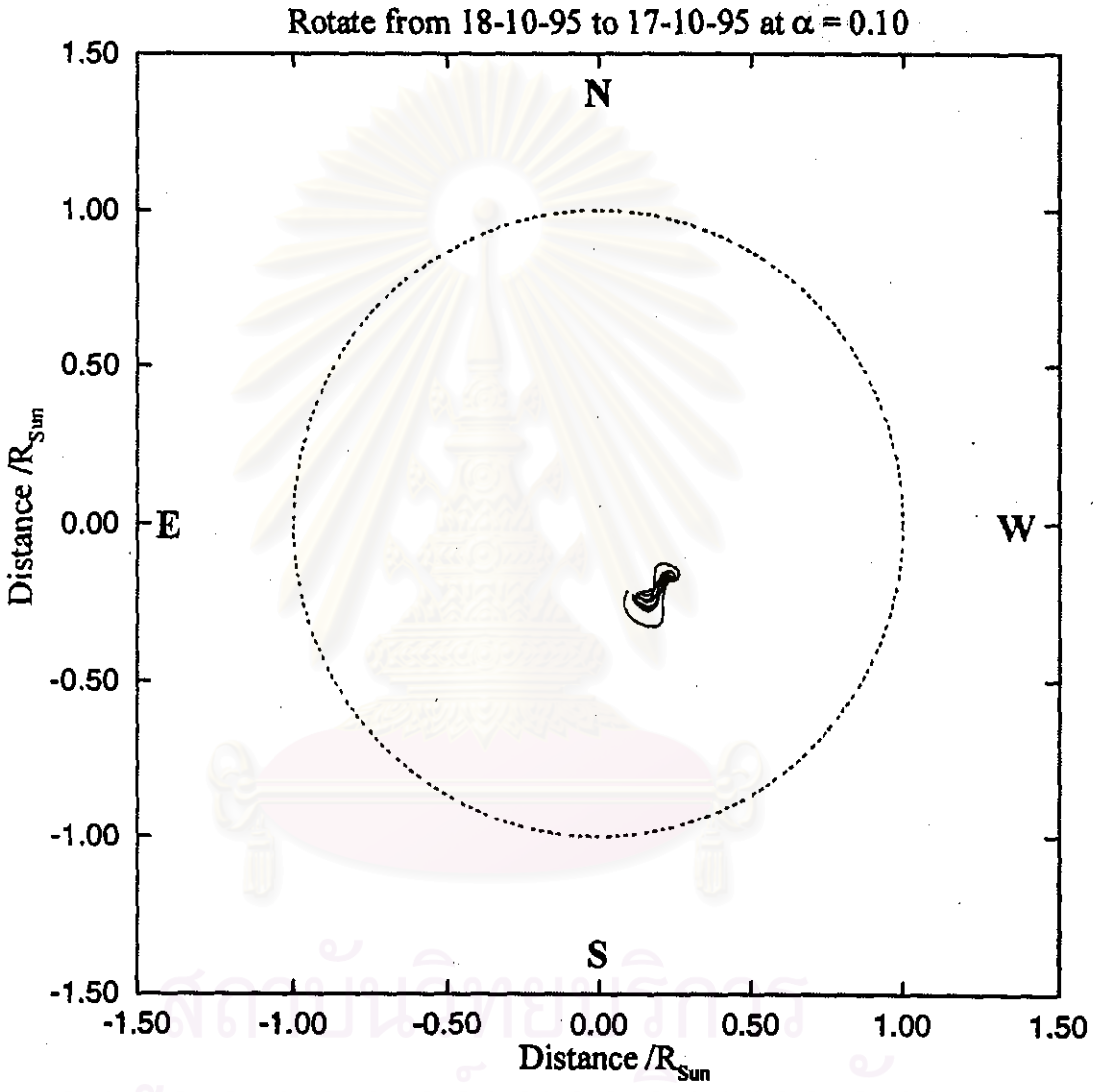

Figure 5.30: Simulation of the magnetic field, rotated from 18-10-95 to 17-10-95, at $\alpha = 0.10$ arc second^{-1}.

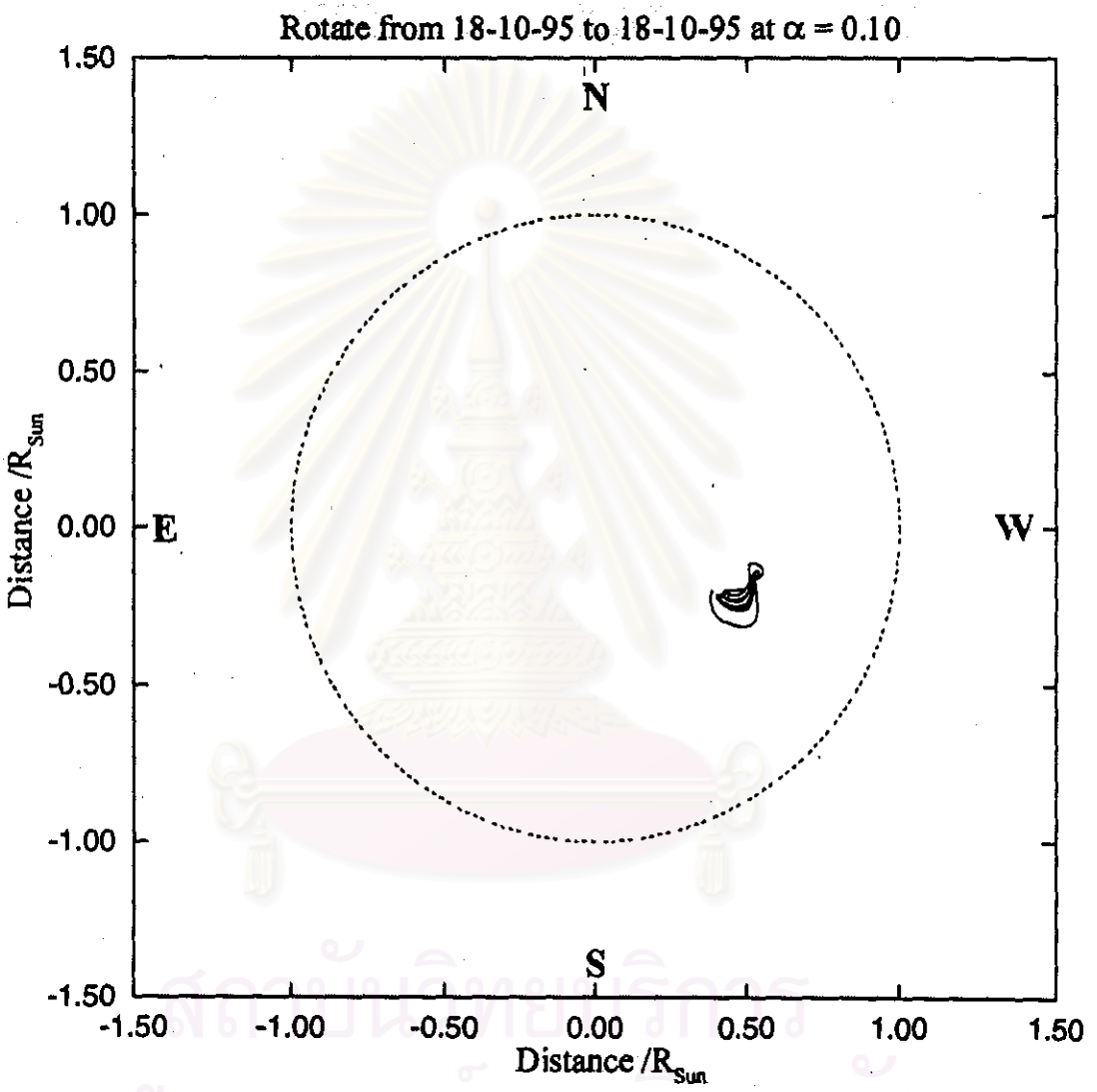

Figure 5.31: Simulation of the magnetic field, rotated from 18-10-95 to 18-10-95, at $\alpha = 0.10$ arc second^{-1}.

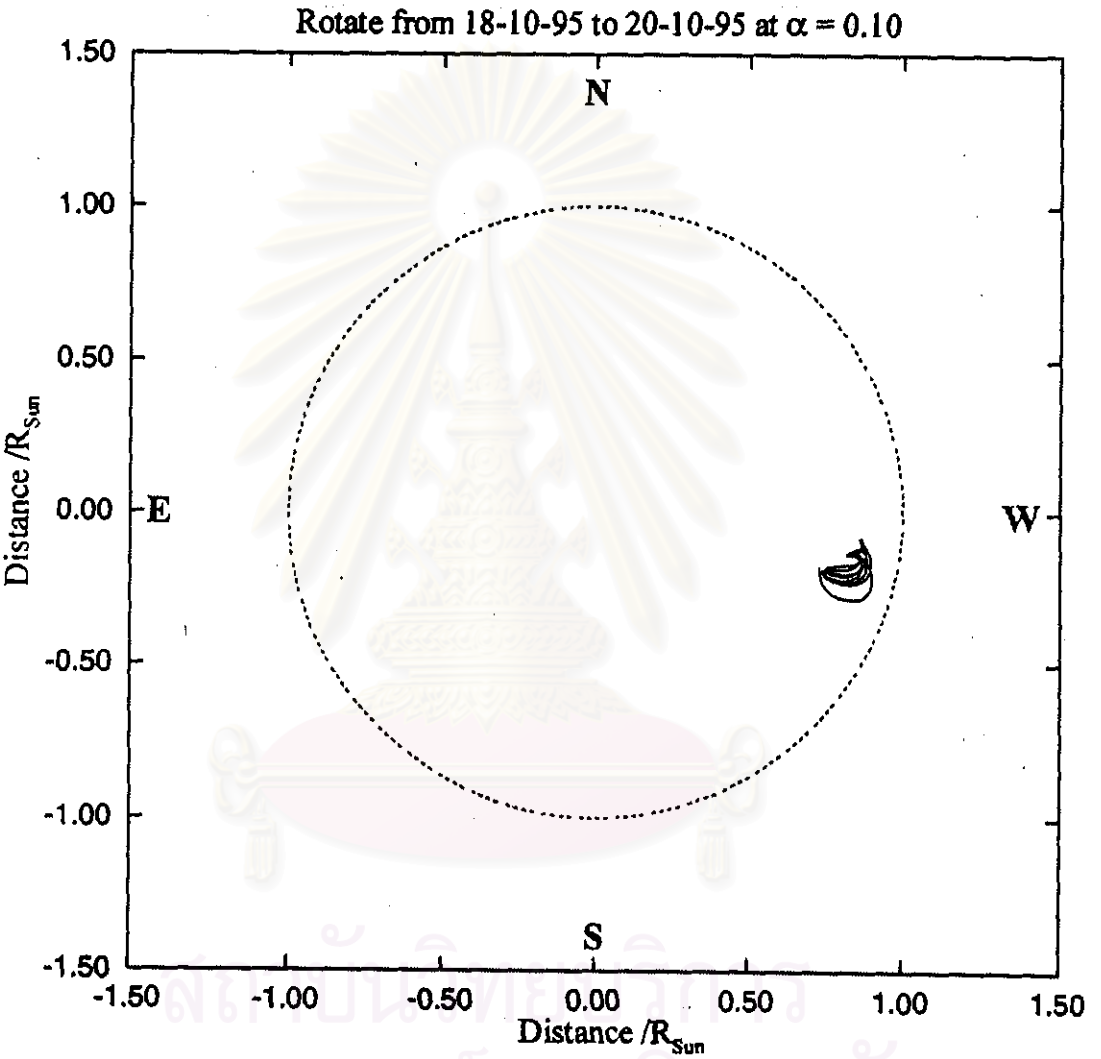

Figure 5.32: Simulation of the magnetic field, rotated from 18-10-95 to 20-10-95, at $\alpha = 0.10$ arc second^{-1}.

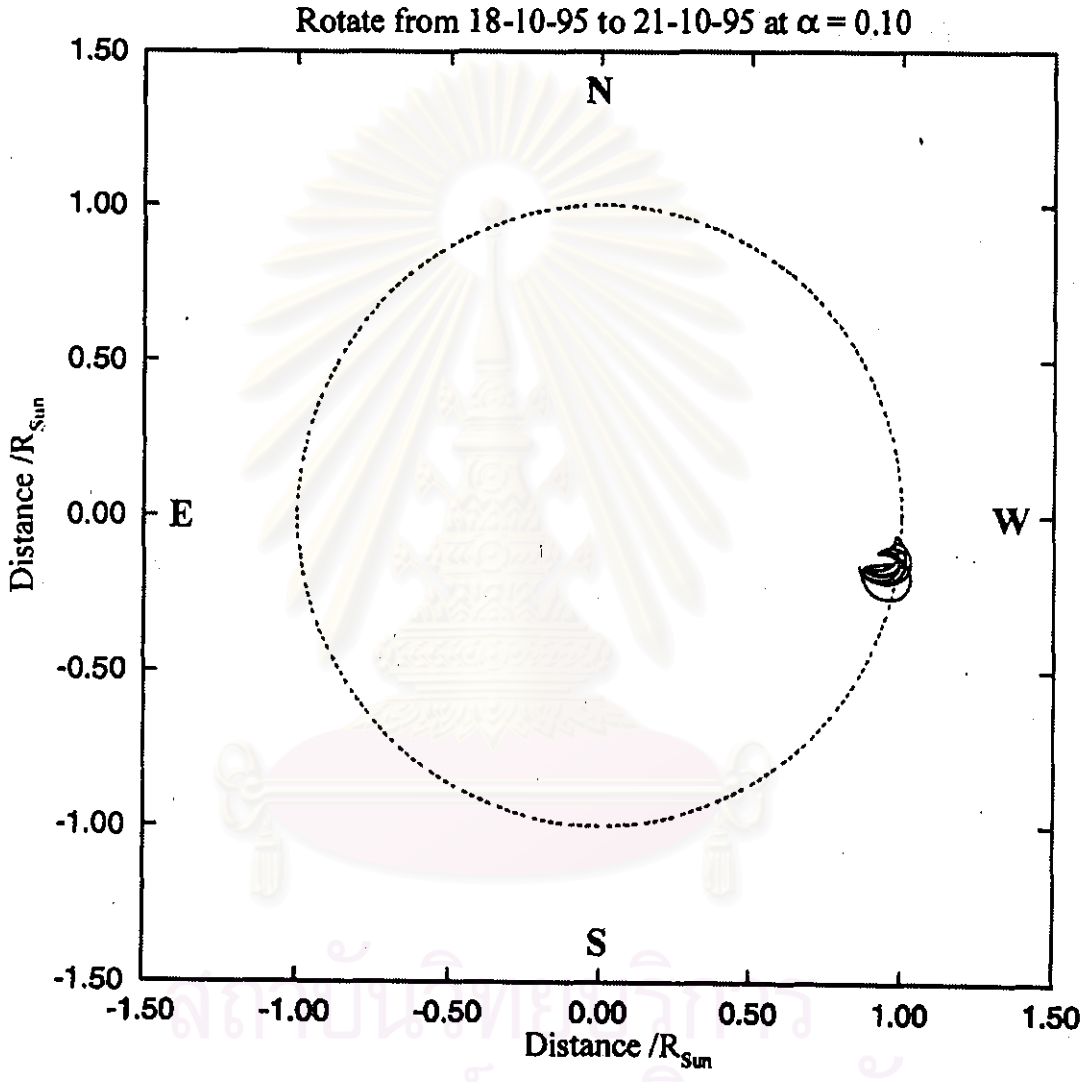

Figure 5.33: Simulation of the magnetic field, rotated from 18-10-95 to 21-10-95, at $\alpha = 0.10$ arc second^{-1}.

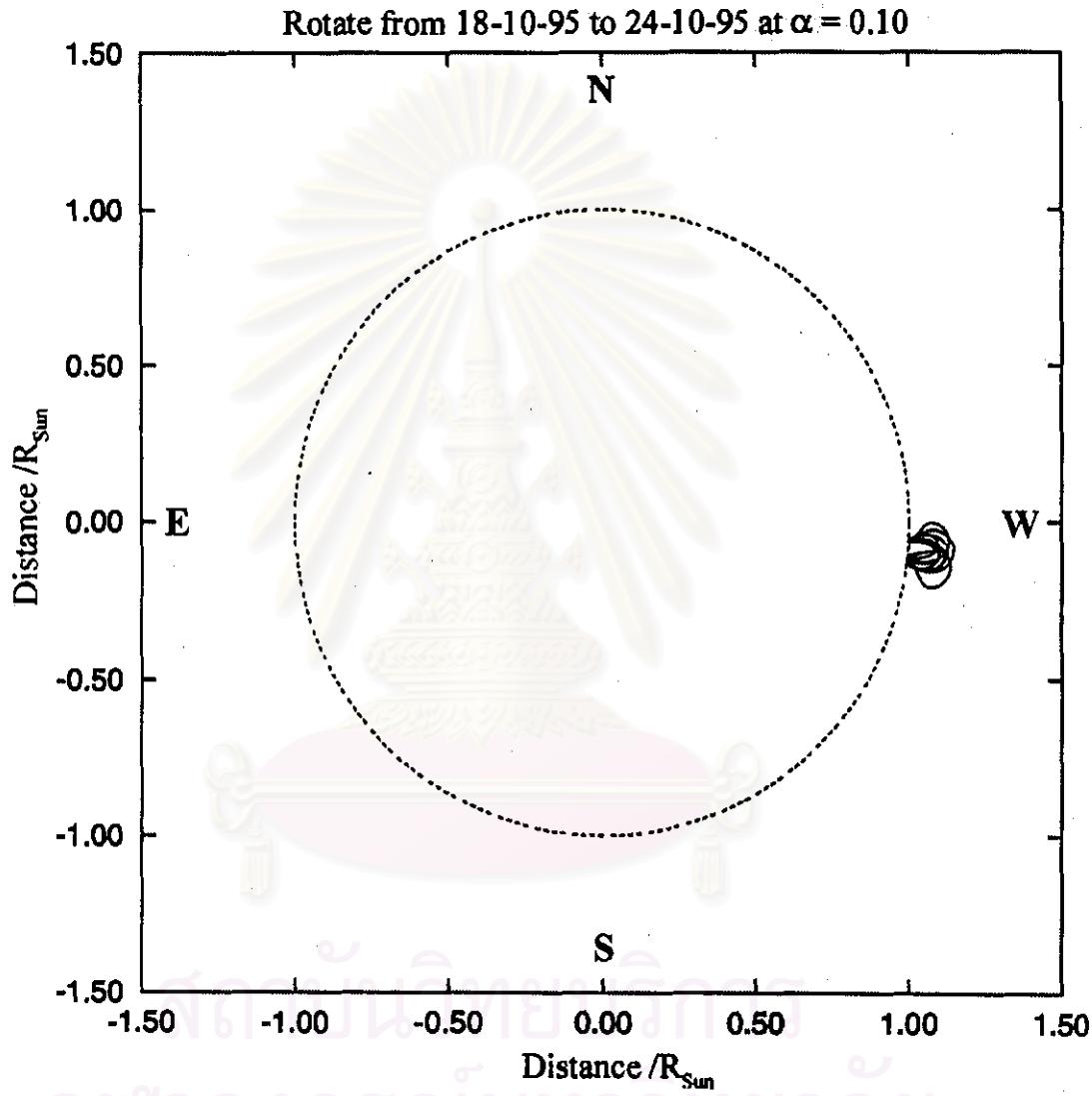

Figure 5.34: Simulation of the magnetic field, rotated from 18-10-95 to 24-10-95, at $\alpha = 0.10$ arc second^{-1}.

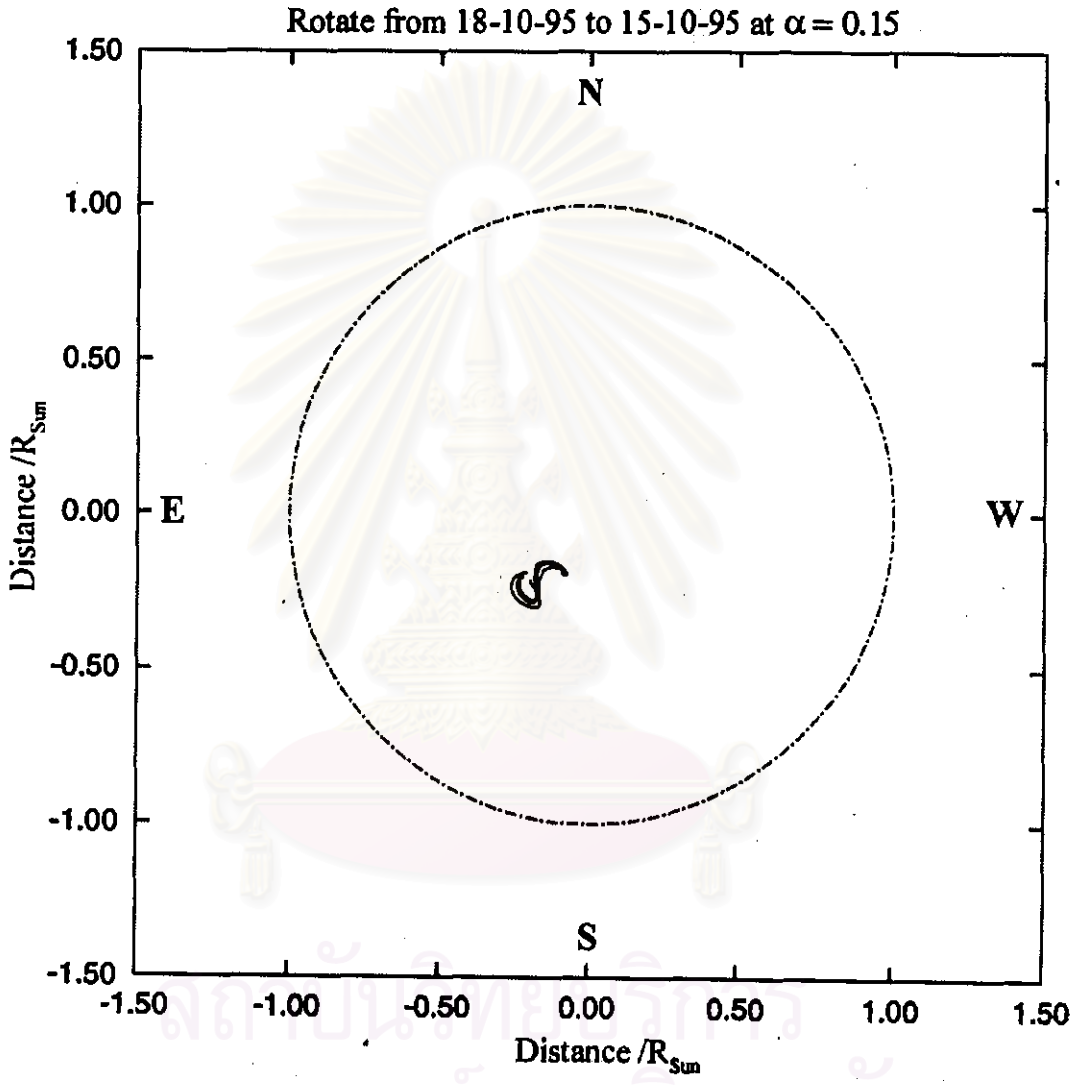

Figure 5.35: Simulation of the magnetic field, rotated from 18-10-95 to 15-10-95, at $\alpha = 0.15$ arc second^{-1}.

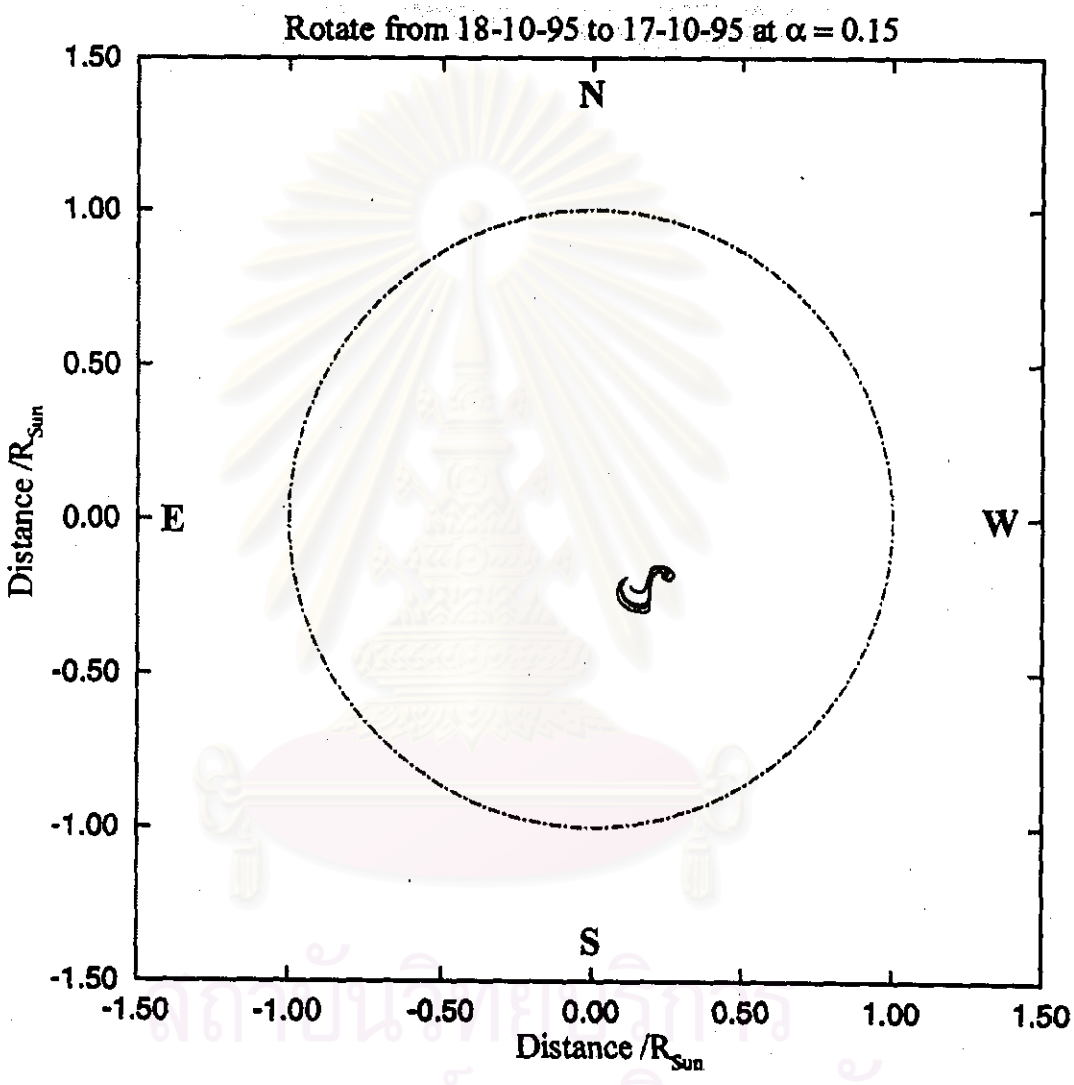

Figure 5.36: Simulation of the magnetic field, rotated from 18-10-95 to 17-10-95, at $\alpha = 0.15$ arc second^{-1}.

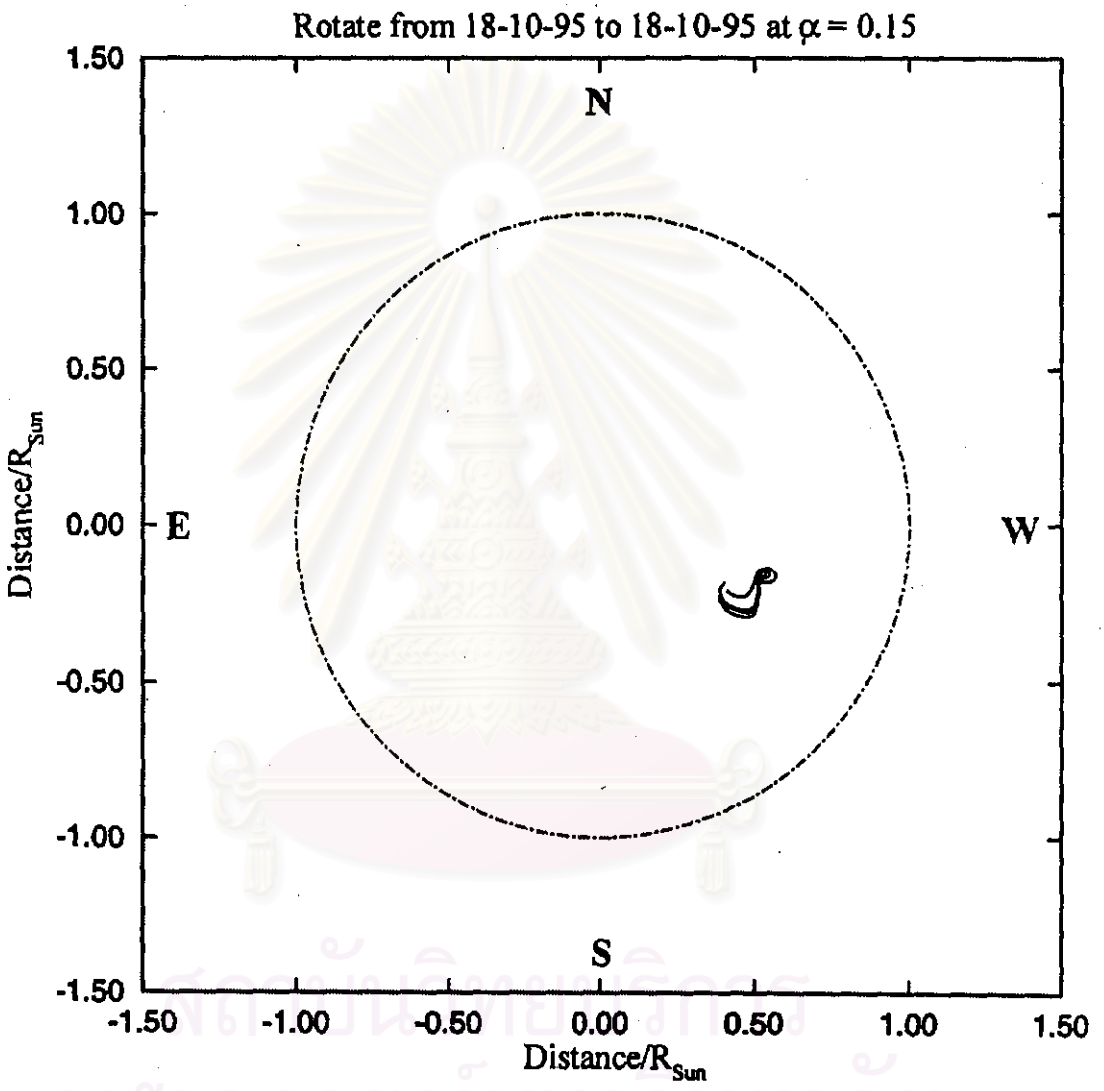

Figure 5.37: Simulation of the magnetic field, rotated from 18-10-95 to 18-10-95, at $\alpha = 0.15$ arc second^{-1}.

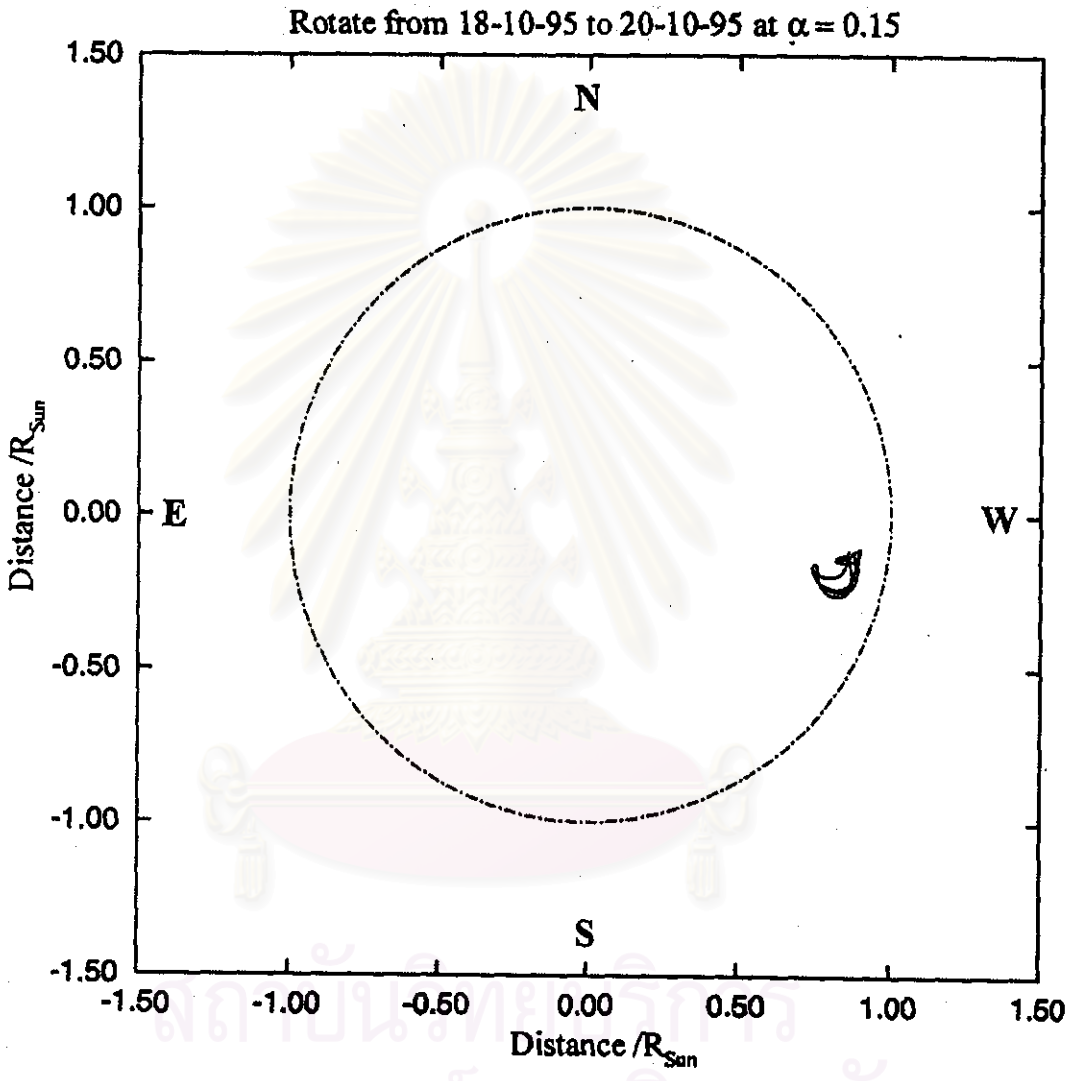

Figure 5.38: Simulation of the magnetic field, rotated from 18-10-95 to 20-10-95, at $\alpha = 0.15$ arc second^{-1}.

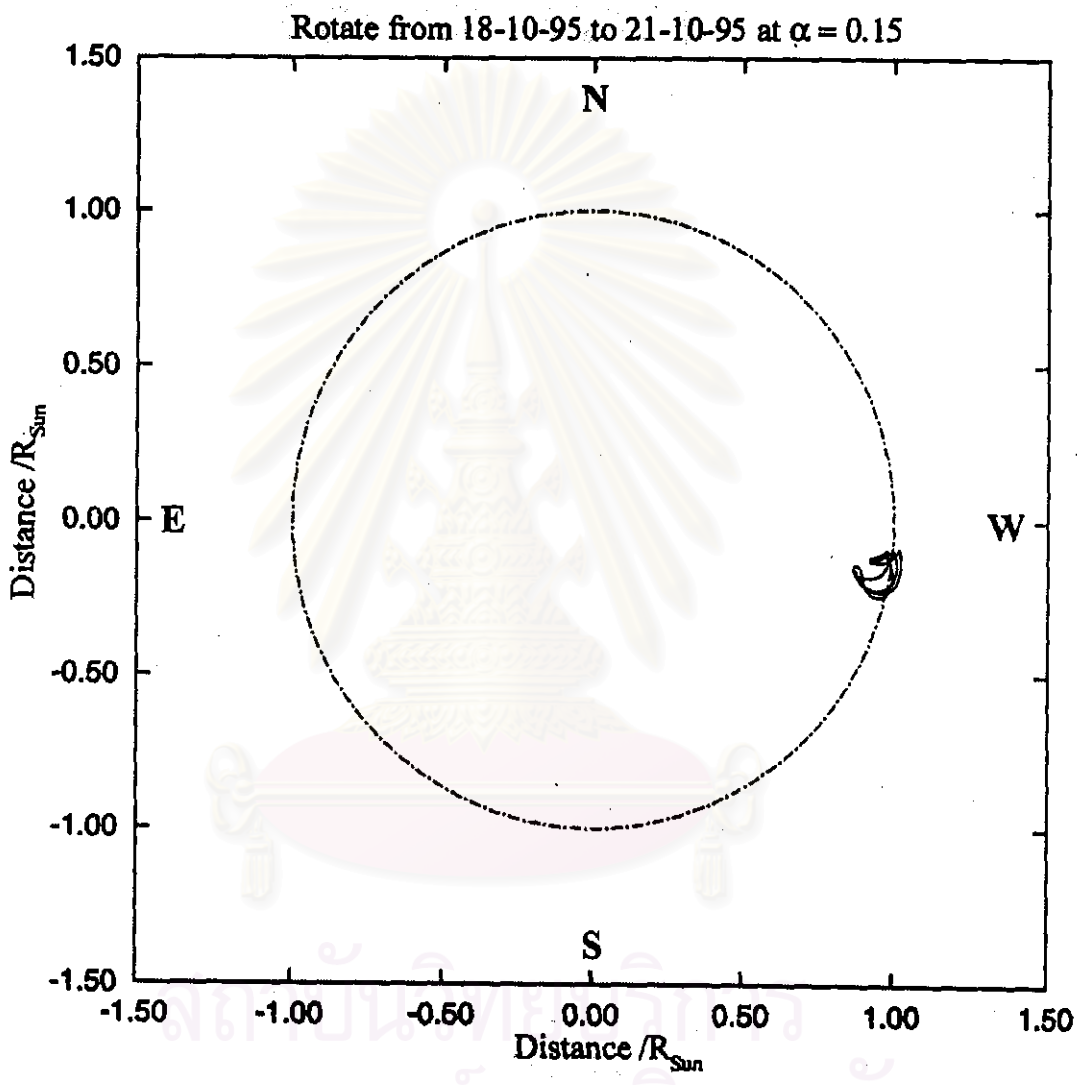

Figure 5.39: Simulation of the magnetic field, rotated from 18-10-95 to 21-10-95, at $\alpha = 0.15$ arc second^{-1}.

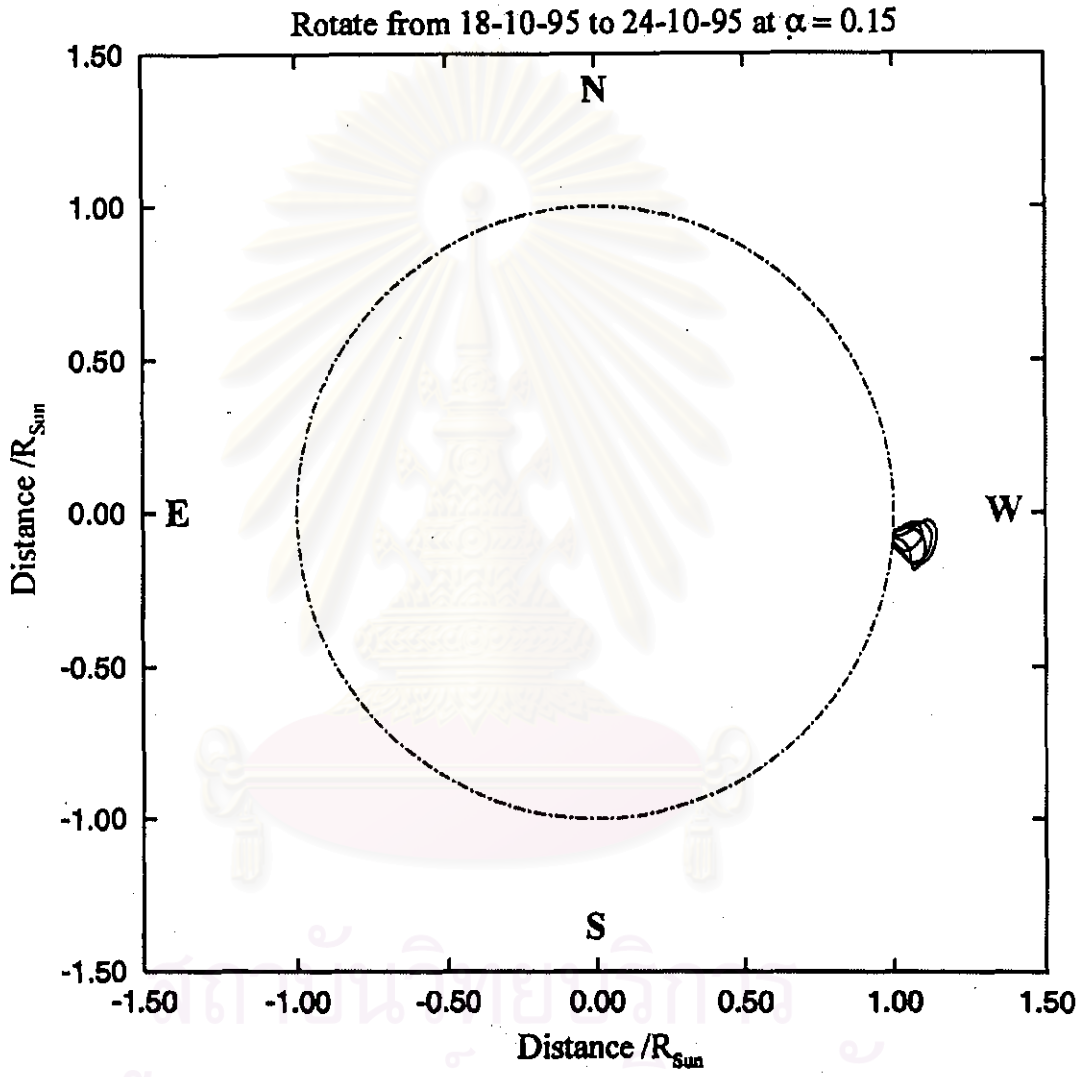

Figure 5.40: Simulation of the magnetic field, rotated from 18-10-95 to 24-10-95, at $\alpha = 0.15$ arc second^{-1}.

5.5 Comparison with Yohkoh Observations

In Chapter III, we showed Yohkoh images in soft X-rays. Here we show one of them to compare with our simulated loop images. This comparison helped us to determine the appropriate value of α. Therefore, for simulated images at different α (0.05, 0.1 and 0.15 arc second^{-1}) for October 17th, 1995, we compared the magnetic field morphology (S-shape) with that of a Yohkoh image in Chapter III (Figures 5.41 - 5.43).

From the comparison in Figures 5.41 - 5.43, we found that $\alpha = 0.1$ arc second^{-1} gives the S-shape as is found in Yohkoh data. Therefore, $\alpha = 0.1$ arc second^{-1} is a suitable value for our simulations.

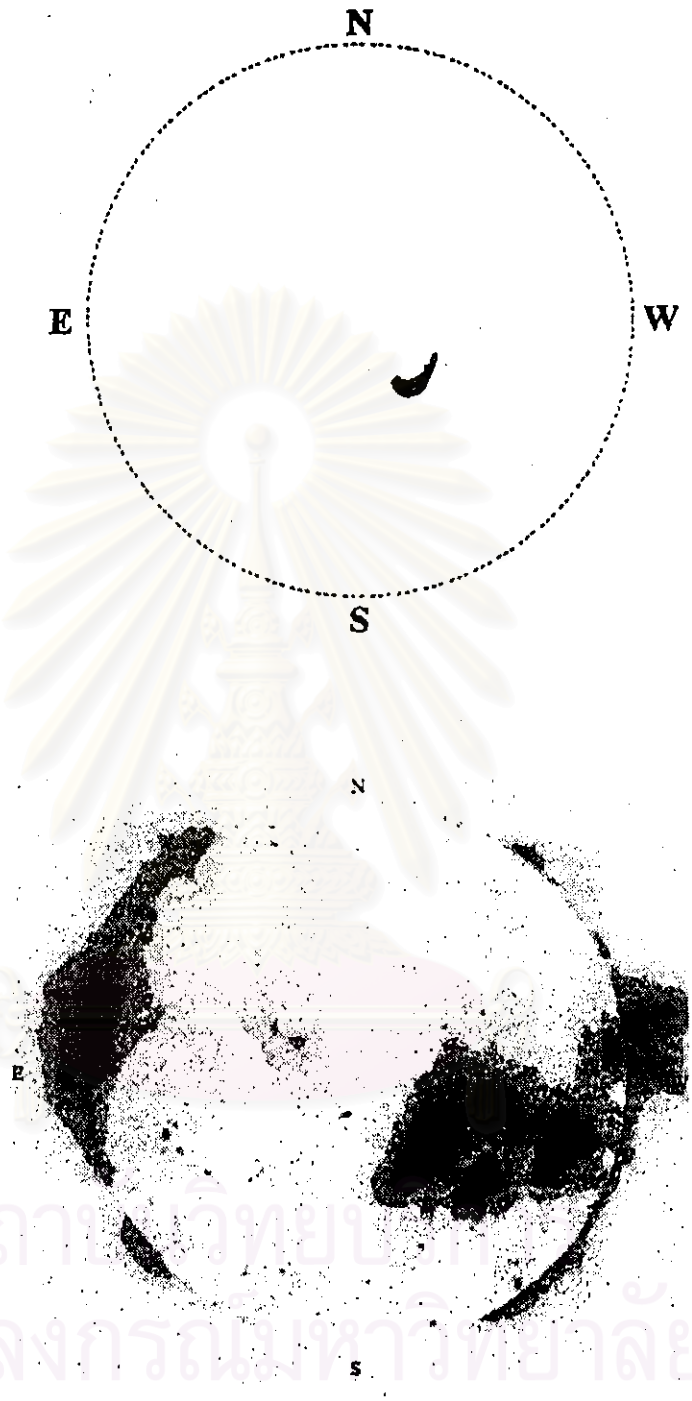

Figure 5.41: Comparison between our simulation at $\alpha = 0.05$ arc second^{-1} and a Yohkoh image for 17^{th} October, 1995.

Figure 5.42: Comparison between our simulation at $\alpha = 0.1$ arc second^{-1} and a Yohkoh image for 17^{th} October, 1995.

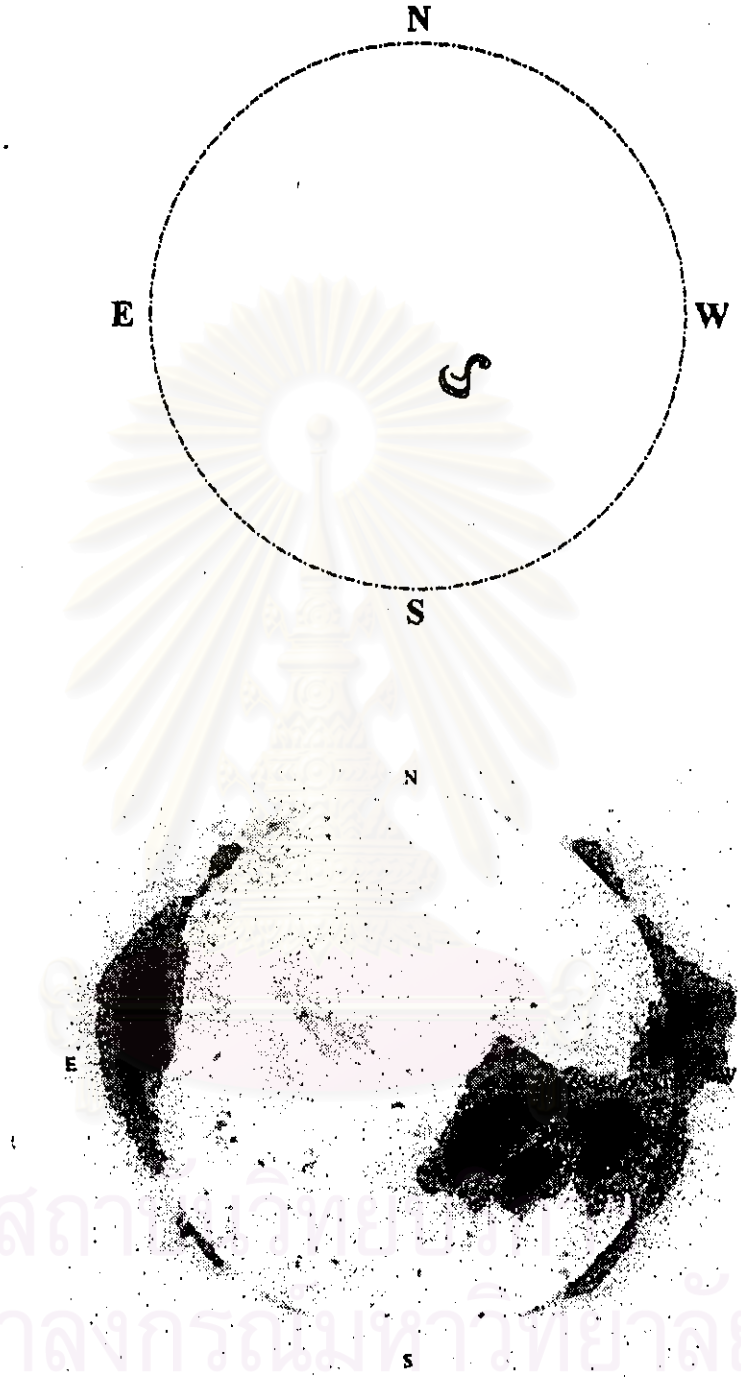

Figure 5.43: Comparison between our simulation at $\alpha = 0.15$ arc second^{-1} and a Yohkoh image for 17^{th} October, 1995.

5.6 Comparison with Chulalongkorn University Observation of the Total Solar Eclipse

We used our simulation for October 24^{th}, 1995 and different α values to compare with the Fe^{+9} image from Chulalongkorn University observations at the total solar eclipse. The field lines in our simulation on October 24^{th} show only the magnetic field structures, not the discontinuity of the plasma in the observed image. This comparison confirmed that the discontinuity in the Fe^{+9} photograph did not occur from small magnetic loops near the footpoints, and the magnetic loop structure indeed contains large ($\sim 10^5$ km) arches with one footpoint at each major sunspot.

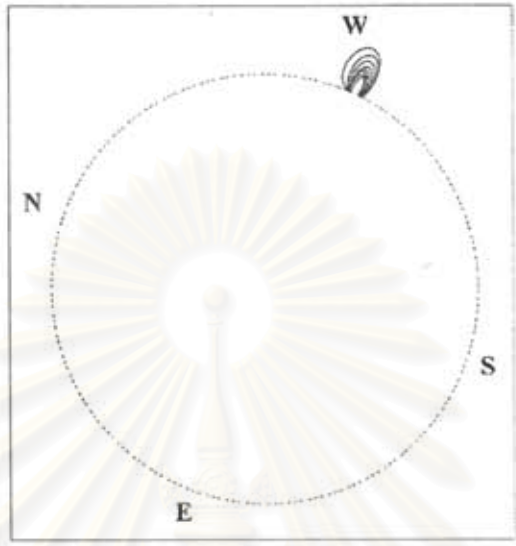

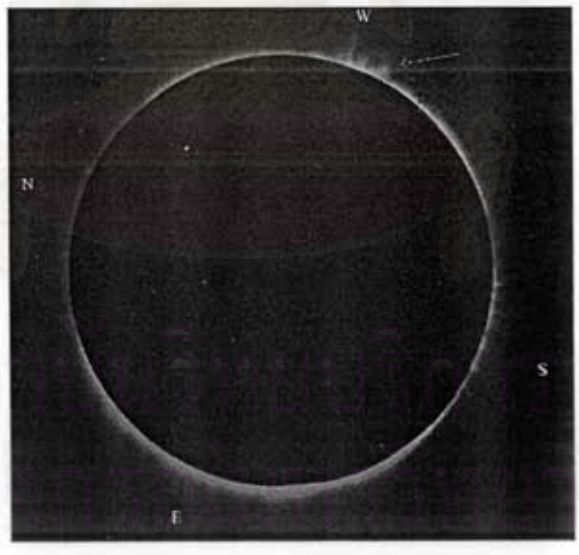

Figure 5.44: Comparison between the simulation result for 24^{th} October, 1995 at $\alpha = 0.05$ arc second^{-1} and the Fe^{+9} photograph from the Chulalongkorn University expedition.

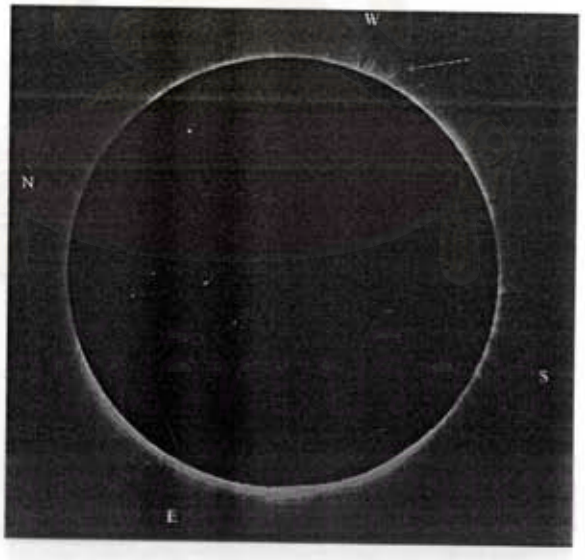

Figure 5.45: Comparison between the simulation result for 24^{th} October, 1995 at $\alpha = 0.1$ arc second^{-1} and the Fe^{+9} photograph from the Chulalongkorn University expedition.

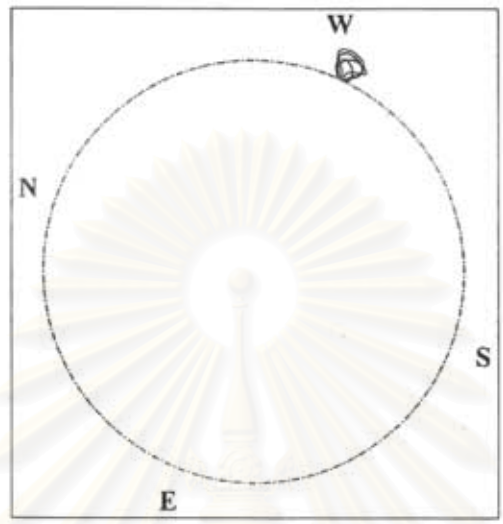

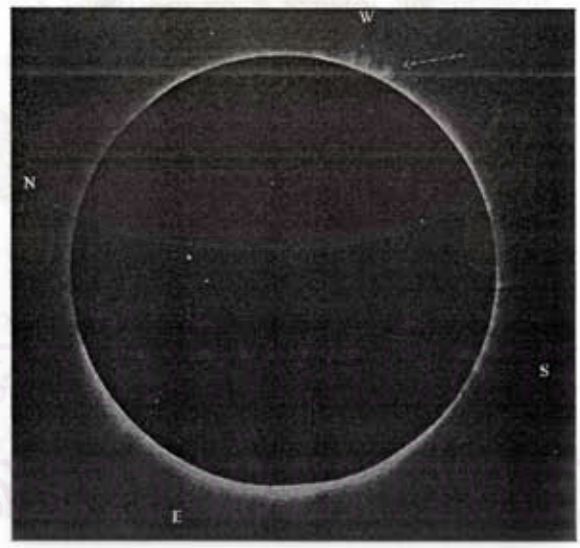

Figure 5.46: Comparison between the simulation result for 24^{th} October, 1995 at $\alpha = 0.15$ arc second^{-1} and the Fe^{+9} photograph from the Chulalongkorn University expedition.